



Recording Pain-Related Brain Activity in Behaving Animals Using Calcium Imaging and Miniature Microscopes

Biafra Ahanonu and Gregory Corder

Abstract

Pain is a multifaceted percept formed by information processing in the brain of ascending signals from the periphery and spinal cord. Numerous studies in humans and animals, using technologies such as fMRI, have demonstrated that noxious stimuli activate a distributed network consisting of multiple brain regions. These human and preclinical studies suggest that the nervous system relays nociceptive information through a vast network of high-order cognitive, motivational, and motor-planning brain regions to generate the perception of pain and resulting nocifensive behavior. While these previous studies have improved our understanding of brain network function in pain, they present limitations due to low-resolution, static snapshots of neural activity, or a difficulty tracking the same cells longitudinally across extended periods of time ranging from weeks to months. Here we present a protocol that uses recent advances in in vivo microscopy and computational techniques to address these questions. Miniaturized fluorescence microscopes (miniscopes) using microendoscopy allow for imaging of intracellular Ca^{2+} transients, which function as a proxy for neural activity. This innovative technology permits high-resolution imaging of large neuronal populations (up to 1000+ neurons in a single animal) located in deep brain regions of freely behaving mice over a time scale of months. This technology puts researchers in a position to answer many fundamental questions regarding the coding principles of nociceptive information and to identify pain-specific neural pathways in the brain. Furthermore, it is now possible to determine how brain neuronal networks evolve their activity dynamics over several months, before, during, and after chronic pain has developed while also understanding how existing and novel analgesics restore both behavior and neural activity to alleviate pain.

Key words Calcium imaging, Pain, Imaging analysis, Behavior analysis

1 Introduction

Pain is a perception. Like all perceptions, it is computed by complex, highly interconnected, and dynamic networks consisting of tens of thousands, if not millions, of neurons in the brain receiving sensory information from the periphery [1]. Different aspects of our perception of pain, for example, the unpleasantness or the sense intensity, can shift or become more salient depending on the environment, time of day, social situations, or our general mood. Such

malleable intensities of how we experience pain indicate that these neural computations fluctuate on a rapid time scale and integrate more than just noxious sensory information into our conscious experiences [2]. This is painfully obviously in pathological pain conditions, where normally protective and necessary pain perceptions arise under completely unnecessary situations and without noxious stimulation [3]. Indeed, we know a great deal about how chronic pain, which affects nearly a third of the population with many patients suffering due to inadequate therapies, can reshape entire regions of the spinal cord and brain as pain becomes less of an evolutionary advantage signal and more of an outright disease of the nervous system [4, 5].

There are many approaches to discovering how the dynamic nature of nociception, or pain-related neural information, is processed in the central nervous system of human pain patients. These range from electrical methods with high temporal resolution, to temporally imprecision but anatomically enlightening whole-brain techniques, such as functional magnetic resonance imaging (fMRI) [6, 7]. Indeed, human physiology studies have been invaluable in providing a detailed roadmap for what regions of the brain are likely to be involved in the different dimensions of our perceptions of pain. However, the resolution of fMRI studies limits interpretation to voxels of activity that represents 100,000+ neurons; thus, the next phase of biomedical and translational pain research will need to improve this functional anatomy by an order of magnitude if one's goal is to identify and disentangle the specific individual neural circuits in the brain that are most critical to generate acute and chronic pain experiences.

There are a variety of existing techniques that allow dissection of neural circuits, but each comes with limitations. Existing approaches to measure activity of individual neurons are limited by only allowing static snapshots of neuronal activity, for example immediate early gene expression [8], or present challenges when attempting to understand the spatial organization of neural activity or track activity, of genetically identified cells, longitudinally over chronic pain relevant time scale of months, such as with in vivo electrophysiological recordings [9]. Further, while head-fixed two-photon calcium imaging circumvents many of these limitations [10], it places the animal in a stressful, constrained environment that may alter pain processing and prevents observation of many ethologically relevant nocifensive behaviors in response to noxious stimuli [11]. Studies aiming to identify functional brain regions—using lesions, chemogenetic, or optogenetic manipulations—likely modulate activity in neural networks unrelated to pain (e.g., those that assign positive valence to stimuli). Similarly, pharmacological approaches often impact functionally heterogeneous populations of neurons. Consequently, how distinct pain modalities are represented in the brain and how neural activity evolves during the

development of chronic pain requires additional precision using new technologies available for preclinical studies in animals.

The advantage of trying to understand nociceptive brain processes in nonhumans, especially rodent subjects, is that an entire new range of invasive imaging technologies have rapidly become available that can provide single-neuron resolution of large networks of neurons across the brain in freely behaving animals. Recent advances in *in vivo* microscopy and microendoscopy, which take advantage of implantable optics, have led to the development of miniaturized fluorescent microscopes (here referred to as miniscopes [12, 13]) that use microendoscopes to image Ca^{2+} transients in neurons and astrocytes (i.e., elevation of intracellular Ca^{2+} that reports cellular activity). These one-photon microscopes permits high-resolution imaging of large neuron populations, up to 1000+ neurons simultaneously [14–16], located in deep brain regions of freely behaving mice over time scales of months. This will prove invaluable in allowing researchers to make conclusions about what type of dynamic network computations contribute to the acute-to-chronic pain transition period along with how neural networks are functionally restored as pain is relieved by existing and novel analgesics. Even more relevant to the pain field, this methodology permits concurrent recording of sensory and affective nociceptive behavior in freely moving animals to uncover the precise neural network coding features that lead to specific behaviors.

Recently, we applied miniscope calcium imaging to one of the first large-scale studies of nociceptive processing in the brain with the aim of elucidating the network computations related to the affective component of pain. In this chapter, we will expand on the technical details for utilizing miniscope imaging and concurrent behavioral analysis for determining the dynamic neural circuit mechanisms of pain in the brain, in a step-by-step protocol with critical considerations for improving this approach in future pain studies to more precisely identify potential nociceptive-specific neural circuits. Many of the procedures, analyses, and techniques described herein can also be applied to non-pain studies of neural activity in freely moving animals.

2 Materials

Materials table located in Table 1. For Ca^{2+} imaging analysis, we recommend users download MATLAB and our calcium imaging analysis software package CIAtah (pronounced cheetah) or calciumImagingAnalysis (CIAPKG) [17], which can be downloaded at <https://github.com/bahanonu/calciumImagingAnalysis>.

Table 1 lists the main materials and equipment that are used to prepare Ca^{2+} indicator expressing mice along with acquiring and analyzing Ca^{2+} imaging movies, behavior videos, accelerometer data, and other experimental variables related to imaging neural activity in mice experience noxious stimuli.

Table 1
Materials used for in vivo imaging of the mouse brain during pain

Items	Product number, vendor, and comments
<i>Animals</i>	
Mice	<ul style="list-style-type: none"> • Wild-type mice. C57BL6/J. Jackson.
<i>Viral injections and implantation surgery</i>	
Cabinets for surgical tool organization	<ul style="list-style-type: none"> • Plastic Small-Parts Cabinet. 9619T61. McMaster.
Waste scavenging, suction, and filtration	<ul style="list-style-type: none"> • Patterson Scientific: EVAC 2—78918181. • Fisher Scientific: Filter Units (50 mm dia.), Millex Inlet and outlet, Pore Size: 0.22 μm, SLFG05010.
Surgery supplies	<ul style="list-style-type: none"> • Cotton tips. • Alcohol, 70% in water. • Betadine (D1415 Povidone Iodine). Dynarex. • 1-mL syringe. • 27G needle. VWR International. • 30G needle. VWR International. • Mammalian Ringers. 50-980-246. Fisher Scientific • Lens Tissues. MC-5. Thorlabs • Biological tape Tegaderm Transparent Dressing. NC9033794. 3M. • Nail polish, black.
Metal cannulas	<ul style="list-style-type: none"> • Custom order of 304S/S Hypo Tube 18X GA. 0495/.0505" OD \times .0410/.0430" ID \times 4.3 mm long; cut and deburred. Ziggy's Tubes and Wires, Inc.
Microendoscopic lenses	<ul style="list-style-type: none"> • 1-mm-diameter gradient refractive index (GRIN) lens. Grintech GmbH. • Lens Probe 1.0 mm diameter, ~9.0 mm length. ID: 1050-004596. Inscopix. • Lens Probe 0.6 mm diameter, ~7.3 mm length. ID: 1050-004597. Inscopix.
Cover glass	<ul style="list-style-type: none"> • Custom order of 2.0-mm diameter cover glass. TLC International (http://www.tlcinternational.com). • Alternative: Small round cover glass, #0 thickness, 3 mm, 100 pack. 64-0726 (CS-3R-0). Warner Instruments.
Surgical tools	<ul style="list-style-type: none"> • Delicate Bone Scraper. 10075-16. Fine Science Tools. • Bonn Micro Probes. 10033-13. Fine Science Tools. • Micro Points. 10066-15. Fine Science Tools. • Bonn Micro Probes. 10031-13. Fine Science Tools. • Dental mirror. B07NZMK31Y. Amazon. • Slotted Screwdriver Set. 5714A4. McMaster.
Headbars	<ul style="list-style-type: none"> • Get headbars custom laser cut or CNC machined, for example from Protolabs, Laser Alliance (San Jose), and other companies. See design in Fig. 3j.
Headbar clamp	<ul style="list-style-type: none"> • C-clamp. CC-2. Siskiyou.
Screws	<ul style="list-style-type: none"> • S/S Machine Screw #000-120 \times 1/16" Flat Head, Slotted Drive. MX-000120-01SFL. Component Supply.

(continued)

Table 1
(continued)

Items	Product number, vendor, and comments
Cement	<ul style="list-style-type: none"> • S380 - C&B METABOND® Quick Adhesive Cement System • S371 - "C" Universal 4-META Catalyst 0.7 mL • S398 "B" Quick Base For C&B METABOND®
Dental cement	<ul style="list-style-type: none"> • Hygenic® Perm, Powder and Liquid Kits. 379-8840. Coltene. • https://www.pattersondental.com/Supplies/ProductFamilyDetails/PIF_52528
GRINjector parts	<ul style="list-style-type: none"> • 3D printed parts, files at https://github.com/bahanonu/GRINjector. • Vernier micrometer. SM-13. Newport. • Bearing stage. 9066-COM. Newport. • Model 1770, Kopf Instruments. For attaching GRINjector to stereotaxic arm. • 2× - 8–32 × 1" cap screw. • 1× - 4-40 × 3/16" cap screw. • 1× - 4-40 × 1/4" cap screw. • 4× - 4-40 × 5/16" cap screw. • Luer lock needle matched to the size of the GRIN lens probe. • 0.5-mm diameter needle that is ~80-mm long.
Drill	<ul style="list-style-type: none"> • Drill. EXL-M40 (http://www.osadausa.com/exlm40.html). Osada. • PS-SC Optical pedestal sliding clamp. Newport.
Micro drill burrs	<p>http://www.finescience.com/Special-Pages/Products.aspx?ProductId=268&CategoryId=126</p> <ul style="list-style-type: none"> • 0.5-mm burrs. 19007-05. Fine Science Tools. For skull screws. • 1.4-mm burrs. 19007-14. Fine Science Tools. For 1-mm GRIN hole.
Micro drill trephines	<ul style="list-style-type: none"> • 1.8-mm trephines. 18004-18. Fine Science Tools.
Optical glue	<ul style="list-style-type: none"> • Optical Adhesive 81. NOA81. Norland Products.
Optical glue curing gun	<ul style="list-style-type: none"> • oGeec 5W Dental Wireless Cordless LED Curing Light Lamp Cure.
UV glue	<ul style="list-style-type: none"> • Light-Activated Adhesive #4305, 1 oz. Bottle. 303389–30769. Loctite.
UV gun	<ul style="list-style-type: none"> • Edmund Optics LED UV Curing Gun NT 59-270 • Alternative: UV Mini Flashlight. 1159N2. McMaster.
<i>Verifying calcium indicator expression</i>	
Peristaltic pump	
Needle	<ul style="list-style-type: none"> • 25G needle.
Curved forceps	<ul style="list-style-type: none"> • Dumont #7 Forceps. 11272-40. Fine Science Tools.

(continued)

Table 1
(continued)

Items	Product number, vendor, and comments
Blunt forceps	• Dumont #5 Forceps. 11295-00. Fine Science Tools.
1x PBS	• Dilute 10× PBS 1:10 in Milli-Q water.
4% formaldehyde	• Dilute formaldehyde 1:10 in 1× PBS
Avertin	• Dilute stock Avertin 1:40 in saline
Histology solutions	• 30% sucrose in 1× PBS • 1x PBS with 0.3% Triton X-100
Serum	• Donkey Serum. 017-000-121. Jackson ImmunoResearch.
Anti-GFP antibody	• a-GFP rabbit at 1:1000 dilution. A11122. Invitrogen.
Anti-rabbit secondary	• DyLight 550 Donkey anti-rabbit 1:500. ab96892. Abcam.
Nuclear stain	• DAPI 50 ng/mL in 1× PBS.
Mounting Medium	• Fluoromount-G™. 00-4958-02. Thermo Fisher Scientific
<i>Checking implant quality and baseplate mounting</i>	
Parts to set up holder for awake animal fluorescence activity checking.	<p>All the below parts are from Thorlabs.</p> <ul style="list-style-type: none"> • BA1S Mounting Base, 1" × 2.3" × 3/8" • MB4 Aluminum Breadboard 4" × 6" × 1/2", 1/4"-20 Taps • PH1.5 Post Holder with Spring-Loaded Hex-Locking Thumbscrew, L = 1.50" • SWC Swivel Post Clamp, 360° Continuously Adjustable • TR4 Ø1/2" × 4" Stainless Steel Optical Post, 8-32 Stud, 1/4"-20 Tapped Hole • TR3 Ø1/2" × 3" Stainless Steel Optical Post, 8-32 Stud, 1/4"-20 Tapped Hole • TR6 Ø1/2" × 6" Stainless Steel Optical Post, 8-32 Stud, 1/4"-20 Tapped Hole • GN2—Small Dual-Axis Goniometer
Rotary encoder.	• BQLZR 600P/R Incremental Rotary Encoder. N04452. Signswise.
Running wheel	• InnoWheel, Catalog No.14-726-577. Fisher Scientific.
Micromanipulator	<ul style="list-style-type: none"> • XYZ Linear Stage, Compact, Dovetail, 0.375 in. Travel, 3 lb., 8-32. MT-XYZ. Newport. • Alternative: XYZ Linear Stage, 0.55 in. Travel, 8-32 & 1/4-20, Triple Divide. 9065-XYZ. Newport.
Miniature microscope holder	• Gripper Part. 1050-002199. Inscopix.
Miniature microscope system	• nVista 2.0 or 3.0. Inscopix
<i>Ca²⁺ imaging experiments</i>	
Miniature microscope system	• nVista 2.0 or 3.0. Inscopix.
Camera lens	• Inesun 6-60 mm 1/3" CS Lens CCTV. B07BTP96RL. Amazon.

(continued)

Table 1
(continued)

Items	Product number, vendor, and comments
Camera	<ul style="list-style-type: none"> • USB 3.0 color industrial camera. DFK 23UP1300. The Imaging Source • Alternative: Guppy Pro F-125 1/3" CCD Monochrome Camera. 68-567. AVT.
Camera trigger cable	<ul style="list-style-type: none"> • Hirose 12-pin female to tinned leads I/O/power cable, 2 m. CB-I/O-02M. 1STVISION INC.
Data acquisition laptops	<ul style="list-style-type: none"> • Aspire 5 Slim Laptop. A515-43-R19L. Acer.
Sensory testing rack	<p>All the below items and catalog numbers are from McMaster:</p> <ul style="list-style-type: none"> • 1× - High-Flow Perforated Sheet Steel, Staggered Holes, 0.03" Thick, 36" Wide × 40" Long. Cut to 12" × 24". 92725T22. • 8× - Aluminum Inch T-Slotted Framing System Four-Slot Single, 1" Solid Extrusion, 2' Length. 47065T101-47065T209. • 4× - Aluminum Inch T-Slotted Framing System Four-Slot Single, 1" Solid Extrusion, 1' Length. 47065T101-47065T411. • 16 - Aluminum Inch T-Slotted Framing System 90 Degree Bracket, Single, 2-Hole, for 1" Extrusion. 47065T236. • 32× - Compact Head End-Feed Fastener, for 1" & 2" W Aluminum Inch T-Slotted Framing System. 47065T142.
Sensory testing equipment	<ul style="list-style-type: none"> • Touch Test (von Frey). 95060-230. Stoelting.
Needle	<ul style="list-style-type: none"> • 25G needle. VWR.
Noise generation	<ul style="list-style-type: none"> • Piezo Buzzer. TDK PS1240. Digi-Key.
Hot stimulus	<ul style="list-style-type: none"> • Hot plate that can reach at least 70 °C.
Cold stimulus	<ul style="list-style-type: none"> • Cooling device that can reach at least 0 °C.
Valve for sucrose	<ul style="list-style-type: none"> • Tube Normally Closed Pinch Valve. 161P011. NResearch.
Lick spout	<ul style="list-style-type: none"> • Reusable Small Animal Feeding Needles: Straight. 7922. Cadence Science.
Aversive odor	<ul style="list-style-type: none"> • Isopentylamine. SKU #126810, CAS #107-85-7. Sigma-Aldrich. • Tissue paper. #05511. Kimtech.
Odor and air delivery	<ul style="list-style-type: none"> • Blood serum tube. 02685A. Fisher Scientific. • Valve. MB202-VB30-L203. Gems Sensors and Controls. • Medical-grade compressed air. UN1002.
Open field (circular)	<ul style="list-style-type: none"> • Diameter: 24 in, Thickness: 1/2 in High density VHMW M/M White Opaque. TAP Plastics. • Custom order white Polystyrene sheet. 030" thick, 16" × 96". Mr. Plastics (San Leandro, CA).
Open field (square)	<ul style="list-style-type: none"> • HDPE (High Density Polyethylene) Sheet, Opaque White, 1/4" Thickness, 24" Width, 24" Length. • HDPE (High Density Polyethylene) Sheet, Opaque Off-White, 0.250" Thickness, 12" Width, 24" Length.

(continued)

Table 1
(continued)

Items	Product number, vendor, and comments
Electronics	<ul style="list-style-type: none"> • 3× Arduino Uno. Adafruit. • 1× Arduino Mega. Adafruit. • 3 × 4 Phone-style Matrix Keypad. 1824. Adafruit. • LCD Shield Kit w/ 16 × 2 Character Display. 772. Adafruit. • Electronics Semiconductor Kit. Joe Knows. • Electronics 1/4 W Resistor Starter Kit. Joe Knows. • Breadboard 830 Point Solderless Prototype PCB Board. • Multiwire cable. 2714/5. Daburn Electronics & Cable. Ask if they have left over from normal spool to save money. • Alternative multiwire cable: NMUF5/36-2550SJ. Cooner Wire Company.
Counter-balance arm	• Multi-Axis Lever Arms. SMCLA. Instech labs.
Air Purifier	• HEPA Filter Air Purifier. 895916000851. Germ Gaudian.
Light meter	• Digital Lux Meter. LX1010B. Dr. Meter.
Logic analyzer.	• Logic 8. Saleae. Ask for the academic discount.
Stage micrometer	• Micrometer. 94 W 9910. WARD's Natural Science.
Power meter	• PM100D and S120C. Thorlabs
<i>Imaging and behavior analysis software and hardware</i>	
Imaging analysis	<ul style="list-style-type: none"> • CIAtah or <i>calciumImagingAnalysis</i> (CIAPKG), a calcium imaging analysis software suite. Biafra Ahanonu. • Code and instructions for use can be found at https://github.com/bahanonu/calciumImagingAnalysis.
MATLAB	MATLAB 2018a or above. MathWorks.
ImageJ or Fiji	Download at https://imagej.net/Fiji/Downloads .
Python	2.7 or 3.7
Logic analyzer software	Saleae Logic 1.2.xx data collection software.
Shock software	Freeze Frame, Actimetrics
Analysis workstation	i7 or better CPU with ≥ 64 GB of RAM, ≥ 128 GB SSD, and ≥ 1 TB hard drive.
10 Gb networking	http://www.amazon.com/Intel-E10G41BFLR-Ethernet-Adapter-X520-LR1/dp/B002IYDGMU/ http://www.newegg.com/Product/Product.aspx?Item=N82E16833106066 http://www.amazon.com/Lynn-Electronics-LCLCDUPSM-3M-Yellow-Single-Mode/dp/B008BQ1L2G/
Local server or network attached storage.	Not required, but makes large-scale analysis easier.

3 Methods

This method for imaging and analyzing neural responses to noxious stimuli (Fig. 1) is based on protocols and techniques developed by the Schnitzer and Scherrer groups [18]. The goal of these methods is to enable identification of neurons that encode nociceptive information (Fig. 2) or play a role in nocifensive behaviors. To this end, the procedures here cover the entire protocol from expression of calcium indicators to analysis of neural and behavioral data. In addition, we will highlight the many control experiments and stimuli that allow researchers to gain greater confidence when claiming specificity of neural responses to noxious (painful) stimuli. We will also explain key decision points and reasoning either in the Methods or in the associated Notes.

Prior to starting any calcium imaging analysis experiment, it is prudent to investigate whether prior publications have performed Ca^{2+} imaging in the brain region(s) you wish to investigate. This will be particularly useful for determining which gene delivery strategy, stereotaxic coordinates, and control stimuli to use and delivery.

Throughout the methods, we give coordinates as anterior-posterior (AP), medial-lateral (ML), and dorsal-ventral (DV) from bregma, unless specified otherwise (e.g., we sometimes measure DV from dura). For all coordinates, negative AP, ML, and DV indicates left, caudal, and ventral from bregma. These coordinates can be verified by checking the widely used Paxinos and Franklin reference mouse atlas [19].

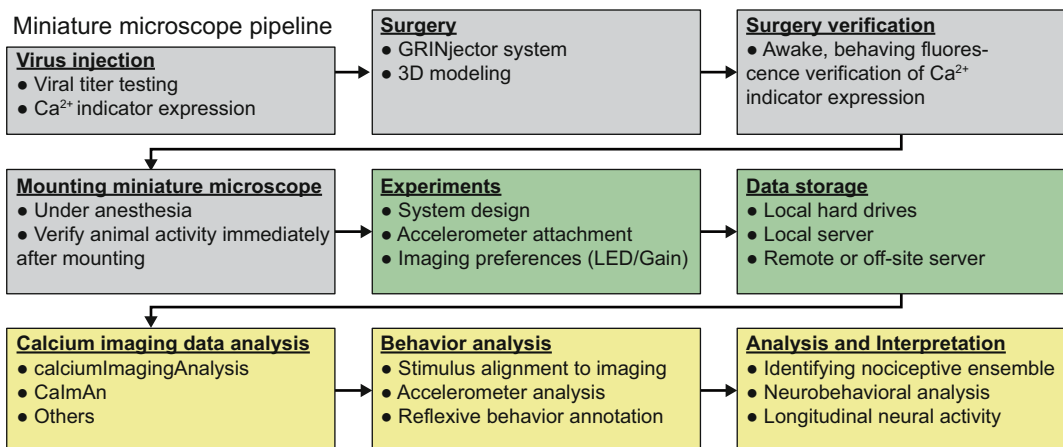


Fig. 1 Overview of calcium imaging pain experiments. Outline of the major steps to conduct pain-related brain calcium imaging experiments. Grey, steps to express virus and verify imaging. Green, pain-related brain imaging steps. Yellow, post-experiment data analysis and interpretation steps

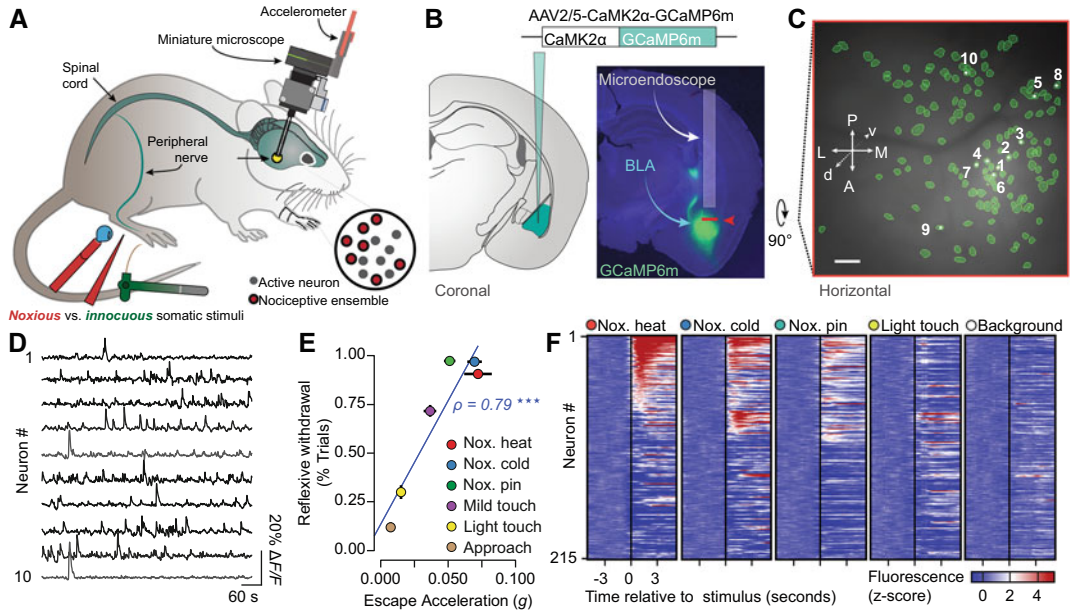


Fig. 2 Overview of calcium imaging and analysis of pain. **(a)** Neural activity is imaged in freely behaving mice with a microendoscope and the virally expressed fluorescent Ca^{2+} indicator, GCaMP6m. Noxious mechanical (pin prick) and thermal (55°C H_2O and 5°C H_2O or acetone) stimuli are delivered to the left hind paw, while reflexive and affective-motivational behavior are monitored via a scope-mounted accelerometer. **(b)** Microendoscope placement and GCaMP6m expression in the right, contralateral BLA. **(c, d)** Map of active BLA neurons ($n = 131$ neurons) with numbers in **(c)** matching PCA-ICA derived neuron activity traces in **(d)**. Scale bar, $100\ \mu\text{m}$. **(e)** Spearman's correlation between reflexive withdrawal and affective-motivational escape acceleration. **(f)** Mean Ca^{2+} response (Z-scored $\Delta F/F$ per trial) across all trials for all BLA neurons imaged during a single session ($n = 215$ neurons). Neurons are aligned from high to low Ca^{2+} responses in the noxious heat trials. Individual neuron identifications between different stimuli are consistent across the trial rows

3.1 Animals

Ensure that you have approval for the procedures described in these methods from your institutional Administrative Panel on Laboratory Animal Care, as these procedures required multiple survival surgeries over several weeks. We recommend housing mice 1–5 per cage and maintaining them on a 12 h light–dark cycle in a temperature-controlled environment with ad libitum access to food and water. To protect the imaging site, we suggest you singly house animals that have had the miniature microscope baseplate mounted and/or are undergoing active Ca^{2+} imaging experiments. For experiments involving imaging at a single brain location, use C57Bl/6J mice (Jackson Laboratory, stock #664, male), or strains of comparable size and weight, at 8–12 weeks at the start of experiments.

3.2 Viral Injection and Expression of Calcium Indicators in Specific Brain Regions

The below are general steps to take to express a Ca^{2+} indicator in rodents (Fig. 2b). Please follow specific protocols as detailed in your lab's Administrative Panel on Laboratory Animal Care (APLAC) or Institutional Animal Care and Use Committees (IACUC) approved protocols.

1. Conduct all surgeries under aseptic conditions with glass bead sterilized surgical tools (Dent-Eq, BS500) after autoclave sterilization (follow institutional guidelines). Prior to surgery, clean and disinfect the surfaces upon which you will perform the surgery or place sterile surgical tools. Wash hands with disinfectant and don sterile gloves.
2. Anaesthetize mice with gaseous isoflurane in O₂ (2–5% induction) until they no longer respond to a squeeze of forelimb or hind limb. Alternatively, use a mixture of ketamine and xylazine per institutional guidelines.
3. In a separate area, place a laboratory absorbent sheet and place the animal then clean the scalp and remove scalp hair with either a depilatory cream (Nair) or an electric trimmer.
4. Transfer the animal to a digital small animal stereotaxic instrument (David Kopf Instruments). Anesthetize the animal with isoflurane (1–2% maintenance, do not go above 2% isoflurane unless it is absolutely necessary as it increases the risk of adverse events).
5. For the entire surgery maintain body temperature using a closed-loop rectal-probe heating pad (FHC, DC Temperature Regulation System). Remember to continually monitor the breathing rate and temperature of the animal while keeping the eyes lubricated by a drop of ophthalmic ointment.
6. Inject nonsteroidal anti-inflammatory drug (NSAID) (e.g., carprofen [5 mg/kg] or meloxicam, subcutaneously) as directed by institutional guidelines.
7. Apply lidocaine (0.5%, subcutaneous injection, max 5.0 mg/kg) to the incision site.
 - (a) You can apply a mixture of 2% lidocaine (max 5 mg/kg)—1:100,000 epinephrine (approx. 2.5 mcg/kg) subcutaneously to the incision site, which minimizes bleeding.
8. Clean incision site with 70% ethanol followed by Betadine. Wait a minute then clean with a final 70% ethanol rinse.
9. Make an incision through the scalp at the level of the eyes along the midline for a length of ~1 cm. Retract the skin to expose the surface of the skull and clear the periosteum.
10. Use sterile absorbent eye-spears, or similar sterile absorbent material, to resolve any bleeding at the skull surface. It is also possible to use a blunt tipped needle attached to a vacuum system to dry the skull surface as well.
11. Measure and record the bregma to lambda distance, this can be used to later adjust coordinates for mouse size should you need to improve targeting.

12. Ensure that the brain is level in the dorsoventral and mediolateral axes. This is a *critical* step as tilt in either axes can lead to mistargeting of the final point of reagent delivery. *See Note 1.*
 - (a) Note 1: It is preferable for users to use a dye, such as Fast Green or Methylene Blue, initially to determine that injection coordinates hit their region(s) of interest. This can give results in the same day and will help determine whether the chosen leveling procedure and coordinates will allow you to target the correct brain location. You can test multiple coordinates in the same mouse for structures that are not near the midline by injecting the left and right hemispheres then sacrificing the mice per the procedure outlined in Subheading 3.5.
13. Use a burred drill bit to make a ~0.5-mm craniotomy at your preferred AP-MV coordinates. Set the micro drill to the highest speed and make several successive up-down applications of the drill to the skull surface to gradually remove the skull and to ensure a clean hole is formed with minimal bone fragments. Else make a small incision of the dura over the foramen magnum.
14. Zero needle on bregma, move to AP-MV coordinates, measure and record DV dura distance, and lower needle to DV coordinates. Make sure to slowly lower the needle as this will minimize the chance that the brain tissue under the needle is compressed as it is lowered into the brain.
15. Inject 100–500 nL (recommend 250 nL/min, this will depend on volume and specific compound being injected) of material into the brain. After 5 min from start of injection, raise the needle 100 μ m (modify as needed for brain region and anatomy) for an additional 5–10 min to allow the virus to diffuse at the injection site, and then slowly withdraw the needle over an additional minute, *see Note 2* [19].
 - (a) Material refers to experimental reagents, for example adeno-associated virus, lentivirus, retrovirus, rabies/vsv-g-lenti, or of a fluorescent dye (e.g., Texas red dextran; Calcium Green).
 - (b) We injected using a beveled 33G needle (WPI, NF33FBV-2), facing medially, attached to a 10- μ L microsyringe (Nanofil, WPI) using a microsyringe pump (UMP3, WPI) and its controller (Micro4, WPI).
 - (c) For Ca^{2+} imaging using GCaMP6m (18) in BLA *Camk2a* + principal neurons, we intracranially injected 500 nL of AAV2/5-*Camk2a*-GCaMP6m-WPRE. Care must be taken to ensure that the brain is level in both the dorsoventral and mediolateral axes.

- (d) Note 2: Raising the needle 100 μm will create a small pocket where the injected material can accumulate and minimize backflow. It is very important that you slowly remove the needle from the brain to minimize backflow of reagent along the injection path. This can include moving the needle half-way out of the brain and waiting another several minutes before moving it again slowly out of the brain.
- 16. If you have no additional viral injections planned, rinse the needle used for virus injection in 70% ethanol. Soak in 10% bleach any instruments and material that contacted the virus or the infected tissue for virus inactivation prior to disposal or usual cleaning procedures.
- 17. Suture the skin overlying the injection site (suture size 5-0, single interrupted pattern) or glue with Vetbond as per institutional guidelines. If needed, also suture any neck muscles cut during the procedure (sterile absorbable 5-0 suture, single interrupted pattern).
- 18. Administer long-lasting analgesic (e.g., sustained-release buprenorphine [1.5 mg/kg, subcutaneous injection]) post-operatively, following your institutional guidelines. *See Note 3.*
 - (a) Note 3: If your experiments involve investigations of the endogenous opioid system or related signaling mechanisms, alternative use of a nonopioid perioperative analgesic should be considered (e.g., carprofen or meloxicam) as the opioid may alter endogenous signaling or expression. This can be critical for studies that investigate neural activity before and after chronic pain develops.
- 19. After surgery, let animals recover from anesthesia on a heating pad to maintain body temperature. Provide food pellets in the recovery chamber and inject mice with warm saline (1 mL, intraperitoneal) to improve recovery.

3.3 GRINjector: Fabrication of Lens Probe Injection Device

The GRINjector (Fig. 3d–f) is a device for injecting microendoscopes (microendoscopic gradient refractive index (GRIN) lens probe) into animals that can be used in Subheading 3.4. The advantages are: (1) the injection needle displaces brain tissue, improving targeting and minimizing tissue compression; (2) the GRIN is held in place during retraction of the placement needle from the GRIN and the GRINjector device; and (3) the guide needle can be easily swapped for other guide needles depending on the diameter and length of the GRIN lens probe. We have created a GitHub repository containing computer-assisted design (CAD) files to assist in 3D print necessary parts along with instructions, located at <https://github.com/bahanonu/GRINjector>.

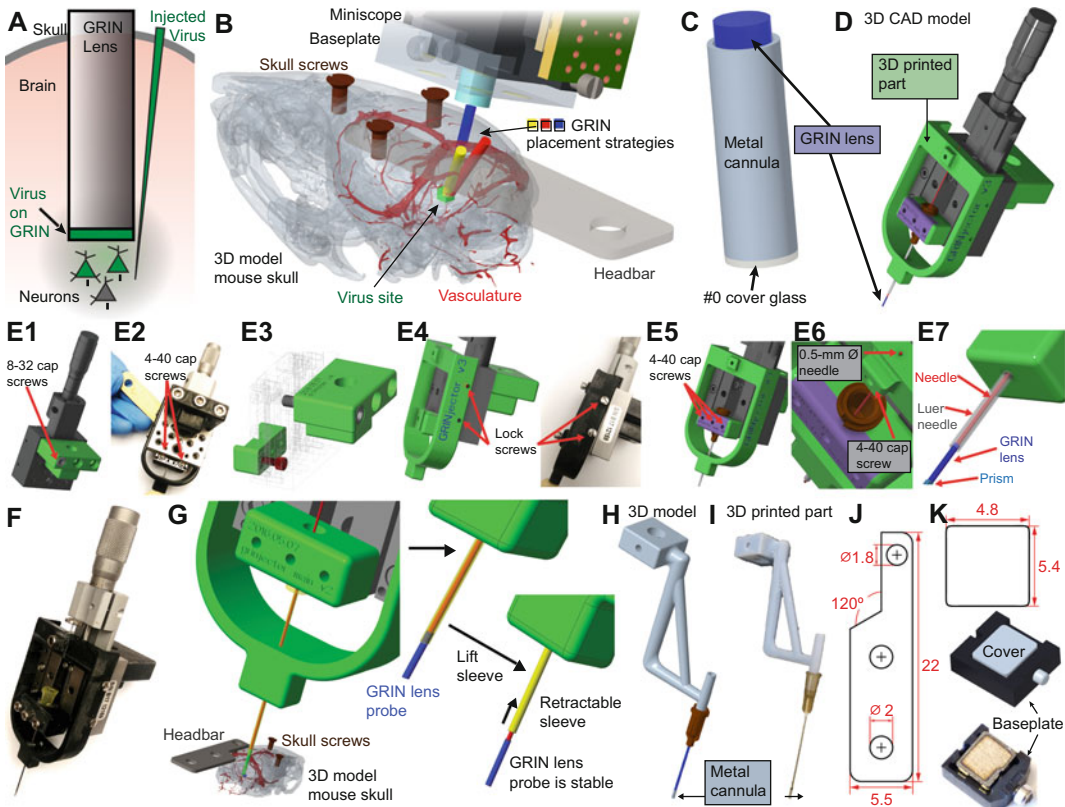


Fig. 3 Implantation and verification of GRIN lens in brain tissue. (a) Diagram of GRIN lens probe placement and virus expression. (b) 3D CAD model of surgery and miniature microscope mounting. Different colored cylinders indicate several potential GRIN lens probe placements to avoid vasculature while still reaching a deep brain region. (c) GRIN lens probe inside a stainless-steel cannula with #0 cover glass glued to the bottom. (d) A custom GRINjector (green, 3D printed parts) was designed in PTC Creo 3.0 around a base (gray) consisting of a Newport Vernier micrometer (SM-13) and bearing stage (9066-COM). A thin metal rod (red) is guided through a blunt needle (yellow) where the 0.6 mm GRIN lens (blue) is held via friction. (e) Step-by-step (1–7) instructions for assembling the GRINjector device. (f) Image of functional GRINjector with 3D printed parts (black) attached to a Kopf Instruments stereotaxic holder arm. (g) Same as in (d). After placement of the GRIN in the correct brain location (here the locus coeruleus), the blunt needle (yellow) is retracted and the fixed in place thin metal rod (red) helps ensure the GRIN does not move from implant location. (h) 3D CAD model of device that holds metal cannula [as in (c)]. (i) Image of actual 3D printed part. (j) Technical drawing (units, mm) of headbar [as in (b, g)]. Units in mm. (k) Technical drawing (units, mm) of laser-cut baseplate cover along with picture of cover in a miniscope baseplate. Units in mm

We provide STEP and STL files for the main parts to allow creation on commonly used 3D printers (Strasys, uPrint, etc.). We recommend printing with a high-resolution (sub-30-micron layer thickness) printer to ensure optimal fit and one with easy to remove support material. We have used VeroBlackPlus on a Strasys Objet30 and found that to work quite well. Below are step-by-step instructions for assembling the GRINjector after printing and obtaining the necessary parts (*see* Table 1).

1. Connect the SM-13 and 9066-COM to form a functional micrometer stage. Remove the locking plate from the 9066-COM as you do not need it as part of the final assembled GRINjector. For help with this, *see* the user manual for more, for example https://web.archive.org/web/20201116023059/https://www.newport.com/medias/sys_master/images/images/he5/h5b/9366526427166/906806B-9066-9067-User-Manual.pdf.
2. Using 8–32 cap screws, connect the Stereotaxic holder attachment to the back of the 9066-COM, connecting to the top-most holes near the micrometer (Fig. 3e1).
3. Next, pull down the bearing stage so that you expose the two 4–40 holes in the back then place 4–40 \times 5/16" cap screws in each hole (Fig. 3e2).
4. Tap the “GRINjector main needle bottom” 3D printed part holes with a 4–40 tap then place it onto 9066-COM as in Fig. 3e3 and screw in the 4–40 \times 5/16" cap screws (red in Fig. 3e3).
5. Align the lock screws that comes with 9066-COM to each of the four holes on each side of the “GRINjector bottom connector” (Fig. 3e4).
6. Next, place a blunt or syringe tip Luer needle whose inner diameter matches or is barely larger than the diameter of your GRIN lens probe into the groove of the “GRINjector main needle bottom” piece then place the “GRINjector main needle top” piece on top of the Luer needle (Fig. 3e5). Screw the “GRINjector main needle bottom” piece in place with 4–40 \times 5/16" cap screws then secure the Luer needle with a 4–40 \times 1/4" cap screw. A syringe (beveled) tip Luer needle allows easier parting of the underlying tissue as you lower the GRINjector into the brain or spinal cord tissue. Note, this setup allows fast swapping of a different Luer needle into the GRINjector, thus enabling use for GRIN lens probes of various diameters.
7. Next, push the Luer needle through the bottom hole in the “GRINjector bottom connector” then obtain a long, 0.5-mm diameter needle and thread it through the small opening at the top of “GRINjector bottom connector” piece (Fig. 3e6). The needle will then go through the Luer needle. Lock the needle in place with a 4–40 \times 3/16" cap screw as indicated in Fig. 3e6.
8. Lastly, verify that the chosen Luer needle fits the GRIN lens probe tightly and that you can push the GRIN lens probe out of the Luer needle smoothly by twisting the SM-13 micrometer (Fig. 3e7, g).

A quick guide to using the GRINjector in animals, detailed more in Subheading 3.4:

1. Attach the GRINjector onto a stereotaxic arm then perform your normal GRIN lens probe craniotomy surgery.
2. Lower the GRIN into the brain using the GRINjector (Fig. 3g, left).
3. After placement at desired coordinates in tissue, raise the blunt tip needle by twisting the micrometer until the needle is clear of the GRIN lens probe. The red needle secures the GRIN in place during retraction of the device (Fig. 3g, middle and right).
4. Secure the GRIN in place with dental cement, UV glue, or your adhesive of choice then after it as set, slowly raise the GRINjector using the stereotaxic arm.
5. If your stereotaxic arm allows angles, you can use the GRINjector to target the same site at different angles to avoid vasculature or vital brain regions (Fig. 3b).

3.4 Microendoscope Implantation

This procedure aims to implant either a microendoscope (microendoscopic gradient refractive index (GRIN) lens probe) into the brain or to implant a cannula (Fig. 3a–i). In the case of the cannula, during later animal experiments you will place a GRIN lens probe inside to image neural activity.

1. Fabricate 1.06-mm-diameter stainless steel cannulas (we custom cut 18G McMaster's 89935K66 to 4.2-mm length pieces at Stanford Varian Physics Machine Shop or ordered 304S/S Hypodermic Tubing 18G custom cut to 4.3-mm length pieces from Ziggy's Tubes and Wires). See Fig. 3c and **Note 4**.
 - (a) **Note 4:** We strongly encourage researchers new to this procedure to attempt the metal cannula implants as the first set of procedures should there be cost concerns. This allows the researcher to conduct dozens of surgeries for a very low cost compared to the thousands of dollars when attempting direct GRIN lens probe implants. All the metal cannula implanted animals can be checked with a single GRIN lens and those that do not meet prespecified criteria for activity in an awake animal can be retired early from the experiment, saving time and money.
2. Attached a 2-mm-diameter 0.1-mm-thick Schott Glass (TLC International, custom order) onto one end of the cannula using optical adhesive (Norland Optical Adhesive No. 81, NC9586074).
3. We ground down the excess glass using a polisher (Ultra Tec ULTRAPOL End & Edge Polisher, #6390) and film (Ultra

Tec, M.8228.1), washed the surface with deionized water, and then placed the completed cannula in a sealed scintillation vial until use during implantation surgeries.

4. We performed stereotaxic implantation of a stainless-steel cannula or microendoscope 1–2 weeks after AAV viral injections. *See Note 5.*
 - (a) Note 5: It is possible to conduct viral injections and implantation procedures in the same surgery, but we advise against this as it leads to a prolonged procedure for the animal, is less efficient due to needing to switch out different equipment. Further, the implantation procedure likely leads to a heightened immune response that may reduce efficiency of viral uptake. Newer approaches allow coating of GRIN lens probes with viral proteins that can allow for single virus plus implant surgery [20].
5. Follow **steps 1–12** in Subheading 3.2 to prepare the animal for surgery and level the skull.
 - (a) For implantation surgeries, anaesthetize mice with isoflurane (2–5% induction, 1–2% maintenance, both in oxygen) and maintain their body temperature using a heating pad (FHC, DC Temperature Regulation System).
6. Remove head hair (Nair, Church and Dwight Co. NRSL-22339-05) and open the mouse skin using scissors or a scalpel.
7. Using a 0.5-mm burr drill bit, perform small craniotomies in three locations. For implant locations caudal to bregma, we often use the following coordinates (ML, AP) unless they are near an implant location: (–0.7, 5.2), (2.1, –3.6), and (–3.1, –3.6) mm. *See Note 6.*
 - (a) Note 6: We often use the drill at maximum speed and do several up down vertical motions to slowly grind away the skull. This minimizes downward force and reduces the amount of skull that will be pushed into the brain. After placing the screws, this leads to two anchor points for the cement on each side of the skull once you implant the GRIN lens probe or metal cannula. Adjust coordinates to achieve the same result should you be implanting in a different area than described here. Alternatively, you can prepare the skull with dentin activator to increase adhesion of cement onto the skull.
8. Screw three stainless steel screws (Component Supply Company, MX-000120-01SF) into the skull until they touch dura. Do not push the screws all the way into the brain.
9. Perform a craniotomy using a drill (Osada Model EXL-M40) and 1.4-mm round burr drill bit (FST, 19007-14). Clean away bone fragments and other detritus from the opening using

sterilized forceps (Fine Science Tools, Dumont #5 Forceps, 11252-20) or curved micro probe (FST, Hook Bonn Micro Probes, 10033-13). Note that some skull bits will have bent themselves into the brain nearly parallel to the surface, make sure all skull bits are removed to reduce chance that the area will become chronically inflamed.

10. Continuously apply mammalian Ringers (Fisher Scientific, 50-980-246) to the surgical area when necessary for the remainder of the craniotomy and implant portions of the surgery. However, after implanting the cannula or microendoscope, it is critical that the skull and surrounding skin is kept dry to improve adhesion of dental cement.
11. Attached a 1.06-mm stainless steel cannula onto a custom designed 3D printed cannula holder (Stratasys Objet30 printer, VeroBlackPlus material, Fig. 3h-i) or place the microendoscope (GRIN) into the GRINjector device (Fig. 3d-g). Both devices are designed to attach into stereotaxic surgery holders (Model 1770, Kopf Instruments). Make sure for the microendoscope that there is enough clearance between the bottom of the probe and the outer metal sheath to be able to lower the entire probe down to the DV coordinates for your brain region.
 - (a) CAD design files (in STL and STEP formats) and instructions for 3D printing and assembling the GRINjector can be found at <https://github.com/bahanonu/GRINjector>.
12. Dip some lens tissue paper in water and set aside to later wipe the lens probe.
13. Zero the bottom-center of the cannula or microendoscope at bregma then move along AP axis until at AP position where implant will take place. This allows the user to be ready for a fast implant after the tissue aspiration and related steps.
14. Prepare two 27-G needles for aspiration by using a digital caliper or ruler to mark the distance you plan to aspirate down to on the needle with a permanent marker. As a secondary check again aspirating past the designated target, bend the needle at the location previously marked. The second needle is a backup in case the first needle becomes clogged during the procedure, which can often occur.
15. To prevent increased intracranial pressure and improve quality of the imaging site, aspirate all overlying tissue down to ~300 μm (0.3 mm) above final implant site using a 27-G needle (Sai-Infusion, B27-50-27G or VWR Cat. No. 89134-172). As you aspirate the tissue, conduct continuous circular motions as you slowly move downward to efficiently remove the tissue and minimize clogging and sudden suction of large amounts of tissue. In our recent study

investigating the basolateral amygdala (BLA) [18], we aspirated down to -4.20 mm (BLA mice) or -2.10 mm (dorsomedial striatum [DMS] mice) from bregma. See **Note 7**.

- (a) **Note 7:** Determining how deep to aspirate is a function of both anatomical and optical considerations. We advise before deciding on the distance above the injection site to aspirate, that you consult the technical specifications for the microscope system and GRIN lens probe that you plan to use along with a mouse reference atlas. For example, many of the Inscopix nVista miniscopes and GRINTECH lens probes they sell have a working distance of $100\text{--}300\text{ }\mu\text{m}$. Due to this, it is advisable to plan to implant the lens probe greater than $200\text{--}300\text{ }\mu\text{m}$ above the desired imaging site. This allows you to account for error in placement and it is in general preferred to be slightly high then implant too deep and risk destroying the desired imaging location.
16. After tissue aspiration, move the cannula or microendoscope to proper AP and ML coordinates then lower until right at dura. Record the DV coordinates then quickly lower down to final DV coordinates. Wait about 10 s then retract the cannula or microendoscope from the craniotomy site, take the wet lens tissue and wipe the bottom of the cannula or microendoscope, and move out of the way of the implant hole. Quickly aspirate away any additional debris or blood that may have been pushed down during the initial implant then rapidly move the cannula or microendoscope back into position and lower down into the brain a final time.
 - (a) This step allows you to remove blood and debris (e.g., bits of skull that were not properly removed) from the bottom of the aspirated hole and thus can improve final image quality and reduce inflammation at implant site. It is possible for very deep brain regions, such as the hypothalamus, that you will want to avoid doing this since it is more difficult to see the bottom of the aspiration hole and reimplantation will likely lead to worse results.
 - (b) For BLA-implanted mice, we lower the cannula to AP: -1.70 mm, ML: $+3.30$ mm (right BLA) or -3.30 mm (left BLA), DV: -4.50 mm. For DMS-implanted mice, we lowered the cannula to AP: -0.80 mm, ML: $+1.50$ mm, DV: -2.35 mm. This placed the cannula $\sim 100\text{--}300\text{ }\mu\text{m}$ above the imaging plan based on the specifications of the GRIN lens microendoscope's imaging side working distance.
17. It is critical at this stage to dry the entire exposed skull and surrounding skin. Ensure that there is no blood leaking out of the implant site. If you cannot stop bleeding from implant site,

surround with a small amount of UV curable glue then cure to seal the implant site. Score the surface of the skull with a bone scraper and apply dentin activator per instructions on your kit.

18. Cover the cannula or microendoscope with adhesive cement (C&B, S380 Metabond Quick Adhesive Cement System), and allowed the cement to set for 2–3 min. Monitor for any blood pooling under the cement as this can prevent it from properly adhering to the skull surface.
19. Place custom designed laser cut headbars (Fig. 3j, LaserAlliance, 18–24G thickness stainless steel) over the left posterior skull screw (Fig. 3b) and applied a layer of dental cement (Coltene Whaledent, Hygenic Perm) to affix both the headbar and cannula to the skull. The cement should evenly cover the entire skull surface and a thin layer of skin near the edge of the incision site.
20. Let the cement dry for 7–10 min before covering the cannula with bio tape (NC9033794 Tegaderm Transparent Dressing), fixing the tape to the cement with ultraviolet (UV) glue (Loctite(R) Light-Activated Adhesive #4305), and allowing the animal to recover from anesthesia on a heated pad. Alternatively, if directly implanting a GRIN lens, cover with the cut bottom end of a PCR tube then cover with bio tape, apply UV glue around the edge of the tape, and cure the UV glue.
21. Monitor the animal daily after the surgery for signs of weight loss or other signs of pain and distress as laid out in your institutional protocols and guidelines.

3.5 Verification of GCaMP Expression in Fixed Tissue

Check viral expression several weeks after injection to confirm both targeting. This involves perfusing the animal, sectioning the brain, and staining for your calcium indicator to enhance sensitivity (Fig. 2b). Skip over this section if your research environment already has established protocols for verifying viral protein expression.

1. Assemble and sterilize tools (e.g., autoclave) according to institutional guidelines.
2. Prime the peristaltic pump with 1× PBS and 3–4% paraformaldehyde (PFA). Then run 1× PBS through the entire line until a small amount comes out of a 25G beveled needle attached at the end.
3. Inject the mouse with avertin (IP, ~1 mL). Alternatively, place an isoflurane-soaked paper towel in an empty mouse cage and place the mouse inside. In both cases, wait for the animal to lose withdrawal reflexes with breathing near cessation.
4. Hold mouse in place by taping or clipping hind paws and forepaws onto the injection apparatus. Cut open the abdomen

and the diaphragm, take care not to damage any organs and especially the heart and lungs.

5. Cut along the ribcage until you almost reach the armpit then clip a hemostat onto the ribcage and pull back to expose the heart. The hemostat helps keep the ribcage from moving back and blocking your view of the heart.
6. Make a small incision along the right atrium of the heart, a small amount of dark red blood should come out.
7. Place a 25G needle into the left ventricle and start the pump to begin perfusing animal with PBS. The fluid exiting from the right atrium should become progressively clearer. Perfuse animal with 20–30 mL of PBS then switch the line to PFA and perfuse the same amount. During perfusion with PFA the animal's tail should twitch and may rise into the air, this is often the sign of a good perfusion procedure.
8. After you have finished perfusing, remove the brain from the skull and fix in 4% PFA overnight on a shaker. Depending on preferred procedure for brain slicing, a day or two after PFA fixation switch the brain to 30% sucrose until the brain sinks to the bottom of the tube.
9. After brains have fixed, place them in 2–4% agarose then cut on vibratome or place them in an OCT compound then cut on a microtome per normal lab procedures.
10. Place brains in a 24 well plate and perform immunohistochemistry as described below.
11. Perform the below immunohistochemistry steps to check expression of GCaMP in your brain region of interest. Using an anti-GFP antibody will help boost detection of low fluorescence GCaMP that might be either have low expression or not be in an active state for a variety of reasons yet would still be visible when imaging. This reduces the chance of false negatives, that is, that you conclude targeting or expression is not sufficient when it in fact is.
 - (a) Wash brain slices three times for 5 min at 25 °C in PBS and 3% Triton X-100.
 - (b) Leave brains in 10% Serum in PBS and 3% Triton X-100 for 60 min. Serum should match species of the secondary antibody.
 - (c) Shake overnight at 4 °C in primary antibody in PBS (Invitrogen a-GFP A11122 rabbit at 1:1000 dilution) with 0.3% Triton X-100 and 1% Serum.
 - (d) Wash brain slices three times for 5 min at 25 °C PBS + Triton X-100 (0.3%).

- (e) Incubate brains for 1–2 h at 25 °C in secondary antibody (e.g., DyLight 549 donkey anti-rabbit at 1:500 dilution) in PBS with 3% Triton X-100 and 1% Serum.
 - (f) Incubate brains with DAPI (50 ng/mL in 1× PBS) for 10–20 min.
 - (g) Wash brain three times for 5 min at 25 °C in 1× PBS.
12. Mount brain sections in PBS on a glass slide then allow the sections to dry. Then wash with distilled water (to prevent crystal formation) and allow to dry again for several minutes. Subsequently, put a layer of mounting medium (Fluoromount-G) over the brains. Use the pipette tip to spread the mounting medium evenly over the brains before placing the glass coverslip on top to reduce the number of bubbles. Store at 4 °C in a dark container until imaging under a confocal microscope.

3.6 Verification of Microendoscope Implantation and GCaMP Expression in Awake, Behaving Mice

Several weeks after implantation, check awake animals for GCaMP fluorescence and Ca^{2+} transient activity on a custom designed apparatus (Fig. 4a, b). Checking in awake animals increases the probability that you will be able to identify animals with appropriate amounts of neural activity, as compared to under anesthesia when many brain regions are silent (Fig. 4c, d).

1. Build the head-fix apparatus, *see* Fig. 4a, uses the parts outlined in Table 1.
2. Head-fix mice by clamping (Siskiyou, CC-1 or CC-2) their headbar and allowed them to run on the running wheel (Fisher Scientific, InnoWheel, Catalog No.14-726-577), which is attached via a custom designed 3D printed part (Stratasys Objet30 printer, VeroBlackPlus material) to a rotary encoder (Signswise 600P/R Incremental Rotary Encoder). *See* Note 8.
 - (a) Note 8: We strongly recommend to avoid using anesthesia either during checking or for any experiments after base-plate mounting as this causes many structures in the brain, such as the amygdala, prefrontal, striatum, etc., to exhibit reduced activity or become silent, which may potentially lead you to classify animals incorrectly as unusable due to lack of neural activity even though their neurons may become active if the animal had been awake. Recent miniscope imaging from Dr. Fan Wang and colleagues has shown that isoflurane and ketamine activates an endogenous analgesia circuit [21]. Thus, anesthetics might repress signaling in your target area, thereby presenting a false-negative wherein an animal may be inappropriately discarded at this step. Further, repeated anesthesia is reported to alter long term neural activity, both passively

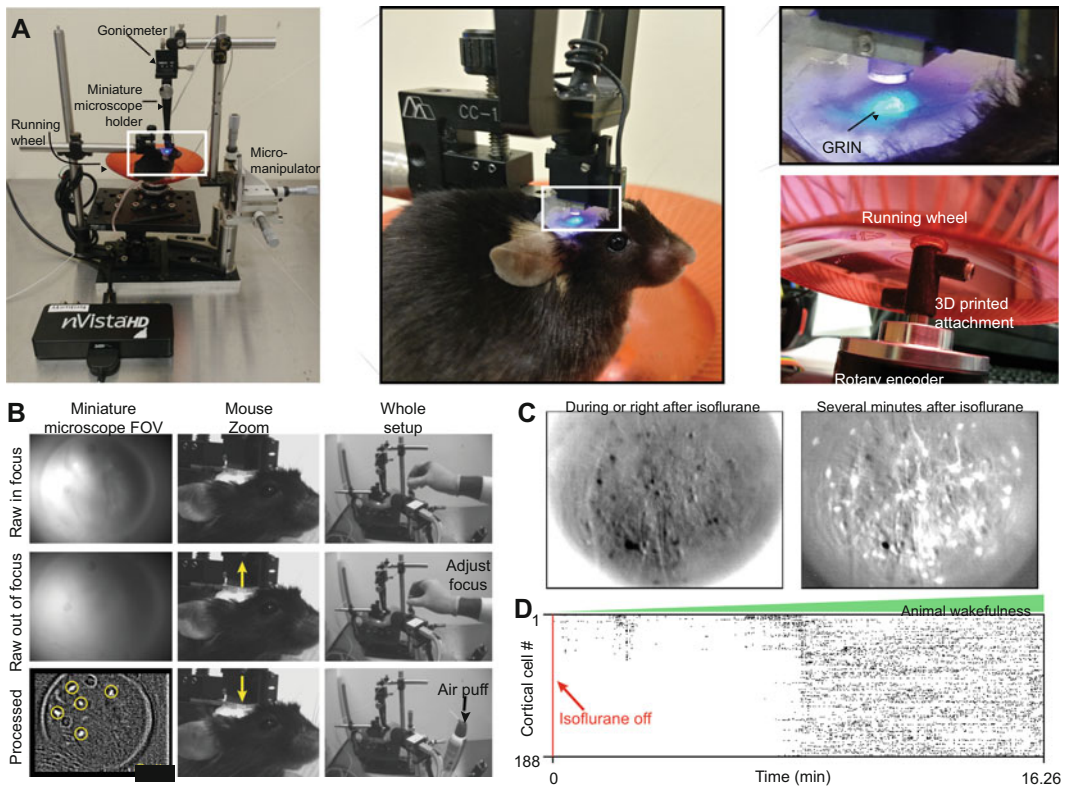


Fig. 4 Verifying indicator expression and experimental arenas. **(a)** Picture of setup to allow awake verification of neural activity in implanted animals. Insets show zoomed in views of the miniature microscope over the GRIN lens probe and an underside view of the running wheel system. **(b)** Example of the miniature microscope field-of-view (FOV) as cells are moved in (top row) and out (middle row) of focus. Bottom row, single frame from an in-focus FOV after calculating $\Delta F/F_0$ showing active cells. **(c)** Example average image (500 frames each) showing activity of frontal cortex neurons during or right after isoflurane anesthesia and several minutes after anesthesia when the animal is more awake. Note the marked difference in neural activity. **(d)** Same animal as in **(c)**, showing neural activity rasters from Ca^{2+} transients extracted from the entire over 16-min (4878 frames at 5 Hz, downsampled $10\times$ for visualization) movie. As can be seen, there is little activity right after isoflurane is turned off, which mirrors activity during anesthesia. This hinders evaluation of whether an animal has sufficient cells to proceed to imaging

and in behavioral tasks; thus, keeping the number of times an animal has to be anesthetized to a minimum is paramount for obtaining accurate and reproducible data.

3. If you implanted a cannula, use a forceps, or a 27G needle attached to a vacuum line, to lower a custom-designed micro-endoscope probe (1.0-mm-diameter gradient refractive index (GRIN) lens Grintech GmbH) into the stainless-steel cannula.
4. Attach the miniature microscope onto a holder (Inscopix, Gripper Part, ID: 1050-002199) connected to a goniometer (Thorlabs, GN1). The latter allows you to tilt the miniature microscope in x - z and y - z planes to correct for any

misalignment between the implanted and miniscope GRIN surfaces. Connect the holder to a three-axis micromanipulator (Fig. 4a).

5. Use the micromanipulator to lower the miniscope until you see the top of the GRIN surface. To ensure the entire field-of-view will be in focus, adjust the miniature microscope's tilt relative to the microendoscope. Do this by checking that you are level to the GRIN by moving the miniscope in the x - y plane to all four corners of the GRIN surface, if any corners are out of focus make the proper adjustments using the goniometer. This method is easier than trying to adjust by eye.
6. To determine an optimal part of the microendoscope to image neural activity, make minor position adjustments of the miniature microscope in the x - y plane using the micromanipulator until the microendoscope is in the center of the miniature microscope field of view.
7. Begin slowly lowering the microscope until you are in the microendoscope's focal plane.
8. If your microscope allows, use the imaging software (e.g., Inscopix, nVista 2.0 or 3.0) to display incoming imaging frames in units of relative fluorescence changes ($\Delta F/F$) rather than just the raw image. This allows you to observe Ca^{2+} transient activity in the awake behaving mice, especially weak transients that might be hard to see when looking at the raw video if there is high background fluorescence.
9. Check for time-locked responses to both auditory (e.g., hand clap) and sensory (e.g., tail pinch) stimuli. In the raw video, check for any signs of indicator overexpression (i.e., brightly fluorescent neurons lacking Ca^{2+} transient activity). You should mount mice passing both tests with a miniscope baseplate and used for experiments. *See Note 9.*
 - (a) Note 9: Remember to record several videos at a couple of different focal planes that appear to have a fair number of cells. After checking the animal, analyze the videos with CIAtah to determine which focal plan has the greatest number of cells or those with the highest signal-to-noise ratio, whichever is more important for your experiments. Generally, high SNR cells will be easier to find with automated cell-extraction algorithms (such as PCA-ICA [22]) and you will be more likely to track them across days. Save a single frame from this preferred focal plan as you will use this later as a reference when mounting the miniature microscope.

3.7 Miniature Microscope Baseplate Mounting

1. Conduct miniature microscope mounting on anesthetized (2% isoflurane in oxygen) mice that met the criteria described in Subheading 3.6.
2. If you implanted a cannula, carefully drop a microendoscope into the metal cannula. Lower the miniature microscope until you obtain a similar field of view as seen previously with awake verification then remove the miniature microscope and fix the microendoscope in place with UV curable epoxy (Loctite (R) Light-Activated Adhesive #4305).
3. Next, attach the miniature microscope in a manner similar to **step 4** in Subheading 3.6 but instead do so on a stereotaxic animal setup then stereotaxically lowered the miniature microscope, with the baseplate attached, toward the top of the microendoscope until the brain tissue is in focus. Use the imaging session videos taken previously for that animal to obtain the same focal plane where you saw the maximum number of cells or amount of activity.
4. To ensure that the entire field-of-view is in focus, use the goniometer (Thorlabs, GN1) attached to the holder to adjust the orientation of the miniature microscope until it is parallel to that of the microendoscope using a similar strategy as before, that is, focus the FOV on the top of the GRIN lens probe then move the miniscope to the center each of the four corners of the microendoscope. They should all be in focus, if not, use the goniometer to adjust the miniature microscope until all four corners are in focus.
5. Refocus on the desired focal plane where you have previously determined cells are located. During the rest of the mounting procedure, reduce the LED power so you can just barely see the microendoscope or fluorescence, this will ensure that you do not lose the focal plane due to accidental contact with the miniature microscope, animal, or other parts of the stereotaxic stage that can cause the FOV to shift.
6. To fix the baseplate onto the skull, first build a layer of blue-light curable composite (Pentron, Flow-It N11VI) from the dental cement on the mouse's skull toward, but not touching, the baseplate. Try to get it as close to the baseplate as possible.
7. Follow this by placing a layer of UV-curable epoxy (Loctite (R) Light-Activated Adhesive #4305) to affix the baseplate to the composite. Shine UV light on the epoxy for at least 20 s to allow it to cure. To prevent external light from contaminating the imaging field-of-view, coat the outer layer of the composite and UV glue with black nail polish (OPI, Black Onyx NL T02).
8. Before ceasing the procedure, start recording an imaging video of neural activity then remove the mouse from the stereotaxic setup and place them in their home cage with a heating pad

(FHC, DC Temperature Regulation System) underneath the cage. Continue to record activity until the animal has completely recovered then use the system outlined in Subheading 3.6 to remove the miniature microscope. The video collected can be analyzed in CIAtah, which will allow you to obtain an initial sense of how stable the recording is and how many cells you might expect to obtain during experiments.

9. Attach either a provided or custom-designed baseplate cover (LaserAlliance, 16G thickness mild steel, magnetic to allow to snap into baseplate, *see* Fig. 3k) to the baseplate to protect the microendoscope and return the animal to its home cage.

3.8 Miniature Microscope Ca^{2+} Imaging of Pain

We provide a diagram of the experimental setup (Fig. 5) and general outline of the two main experimental imaging sessions and overall pain imaging timeline (Fig. 6). The experimenter should stay in the testing environment throughout the habituation portion of each session to limit variations related to stress and stress-induced analgesia [23]. The main protocol consists of three or four imaging sessions performed on non-consecutive days (e.g., 7, 5, 3, and 1 day(s) before nerve injury or other chronic pain manipulation) to allow time for animals to recover after each imaging session and to reduce photobleaching resulting from long imaging sessions.

3.8.1 Miniature Microscope Behavior Recording Hardware

This section will describe the setup (Fig. 5) to collect and synchronize data from Ca^{2+} imaging, behavior, stimulus timing, accelerometer, and lick detection circuits for animals run through the procedure in Fig. 6. The miniscope acts as the master controller of event timing as we consider time locking to Ca^{2+} activity the most critical aspect of the experiment. We describe two hardware setups for collecting all relevant behavior videos, stimulus delivery times, and accelerometer data: one relies on a set of Arduino microcontrollers and the other one uses two Saleae Logic 8 (SL8 or logic analyzer) along with helper Arduinos. Both use two cameras to record animal behavior (Fig. 5e). It is critical that you test both behavior cameras before running actual experiments by running them for 20–60 min and testing for whether there are any dropped frames relative to the miniature microscope that they are synced to; if that is the case then lower the resolution being recorded at, close unnecessary programs, or remove as many peripherals from the USB hub to minimize possibility that data rate is being interrupted (this is not an issue for IEEE 1394 [FireWire] interfaces).

1. In the first setup (Fig. 5a), which is slightly more expensive but we recommend due to ease of use and reliability, the first logic analyzer measures analog outputs from the miniature microscope attached accelerometer (100 Hz sample rate, *see* Fig. 8),

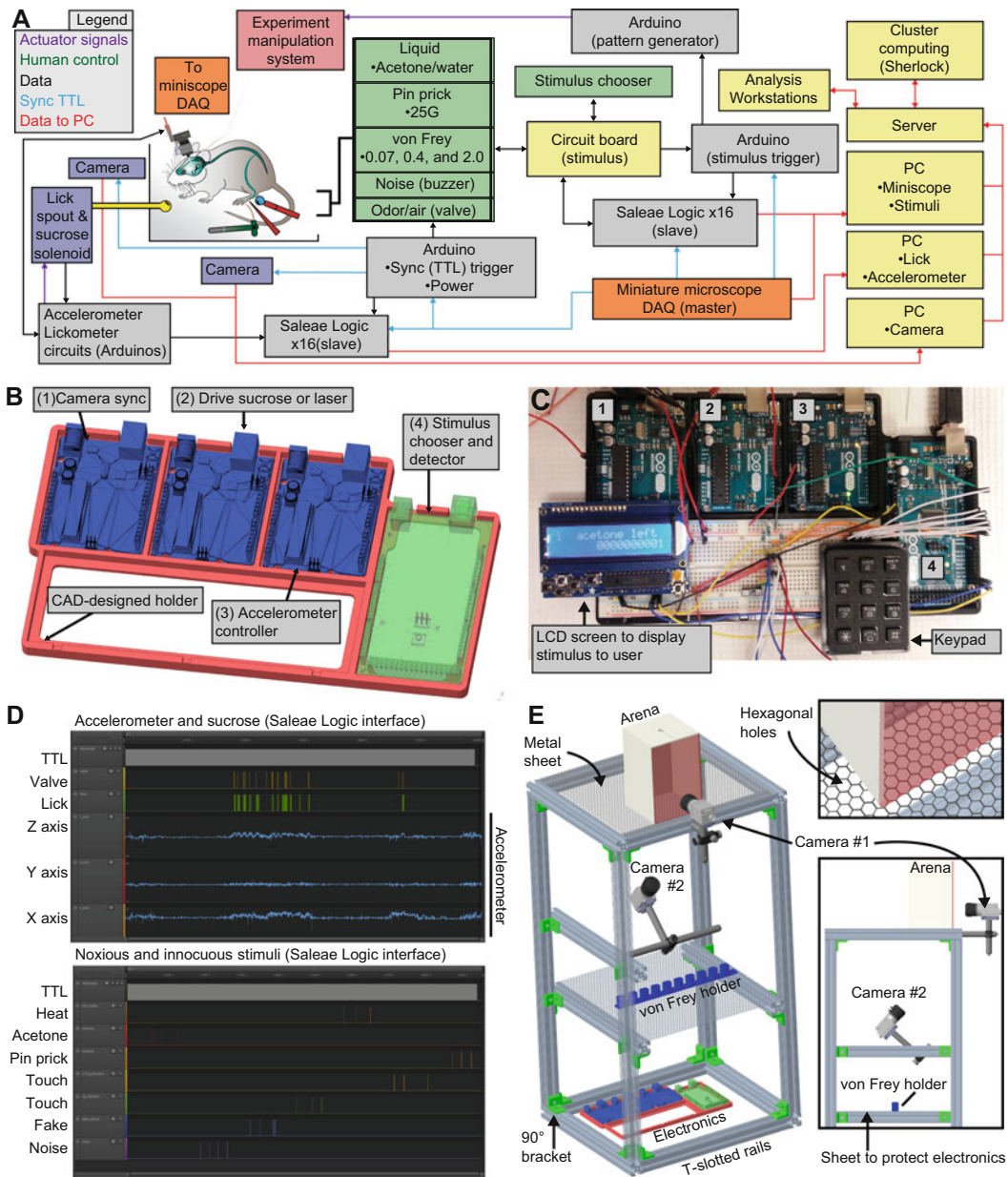


Fig. 5 Experimental setup for synchronous pain imaging and behavior. **(a)** Schematic showing connections between various elements needed to conduct pain imaging experiments with synchronized calcium imaging, accelerometer, lick detection, stimulus application, behavior cameras, and (optionally) experimental manipulation device (e.g., laser for optogenetics). **(b)** 3D CAD model of a holder (red) for several Arduinos (blue and green) used to control various experimental devices [see **(a)**]. **(c)** Example image of Arduinos and stimulus chooser, numbers match those in **(b)**. **(d)** Interface for digital acquisition device (Saleae Logic) collecting experimental variables indicated. TTL is the synchronization trigger pulse from the miniature microscope. **(e)** 3D CAD model of setup used for delivering noxious stimuli while imaging neural activity with the miniscope and recording behavioral responses. Note the second rack with the von Frey holder, by putting an absorbent sheet here you can also protect sensitive electronics or equipment below

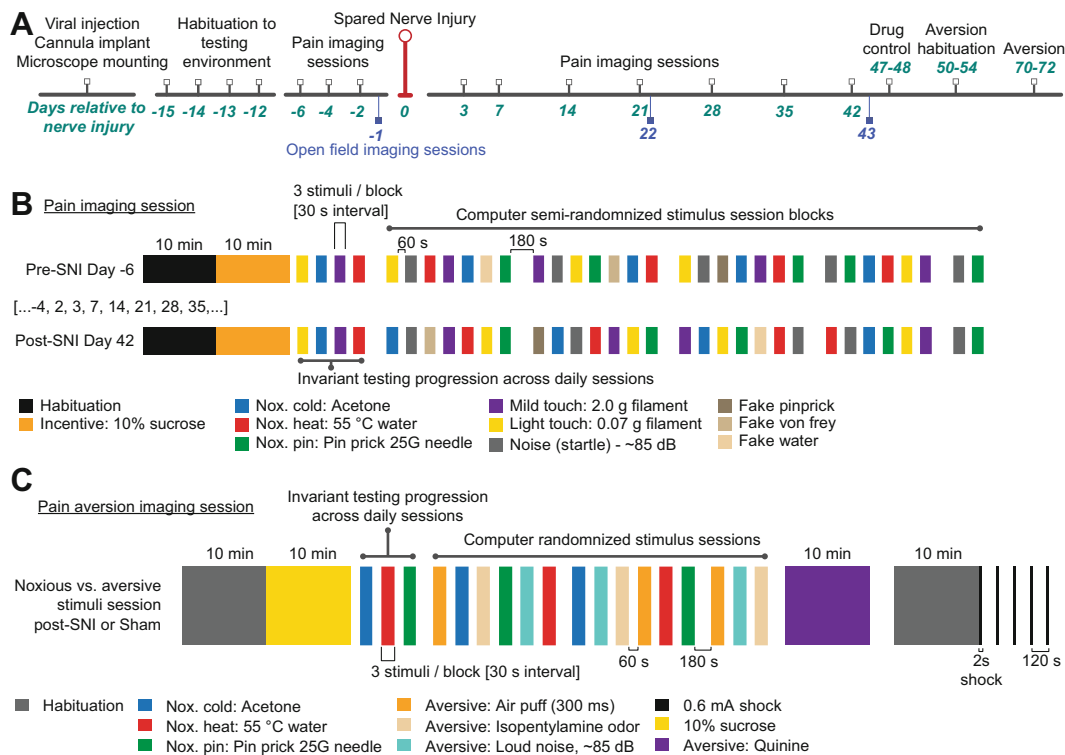


Fig. 6 Outline of pain imaging experiments. **(a)** Experimental timeline and daily imaging protocol for miniature microscope imaged BLA-implanted mice before and after Spared Nerve Injury surgery (SNI). “Drug control” is to check whether neural activity is affected by drug of interest. “Aversion” tested responses of BLA neurons to noxious and aversive stimuli. “Habituation” involved mice being habituated to the fear conditioning chambers used in “Aversion” imaging sessions. **(b)** Each session begins with imaging basal neural activity in the BLA without explicit sensory stimulation (Habituation). Next, mice have free access to a lick port delivering ad libitum 10% sucrose (Incentive), which was removed after 15 min. We then applied somatosensory stimuli to the hind paw. See text for details and explanation of experimental design. During “Approach” trials either a von Frey filament, water droplet, pin, or noise device was moved toward the animal similar to other trials but with no actual contact or stimulus delivery. Open field imaging sessions consist of 30 min sessions of animals exploring a 2 m-diameter circle or 2 m² open field apparatus. **(c)** To compare BLA neuron responses to noxious and aversive stimuli, we study the response of animals to noxious (noxious heat, cold, and pin), five commonly used aversive (air puff [to the face], isopentylamine [odor], loud noise [~85 dB], quinine [bitter taste], and 0.6 mA footshock), and a positive valence (10% sucrose) stimuli

connected via a four- (Daburn Electronics & Cable, #2714/4) or a five- (Daburn Electronics & Cable, #2714/5 or Cooner Wire Company NMUF5/36-2550SJ) conductor wire.

2. Simultaneously, in the same logic analyzer, record timestamps for the onsets of licks and control signals for sucrose delivery (triggered on the rise of each signal pulse to obtain exact timing information). To do this, create a separate circuit consisting of two Arduinos (Uno and Mega) and a custom lick detector [24] that measures the mouse’s licks (signal #1) and sends a control

signal (signal #2) to turn on a solenoid. The first logic analyzer should record both signals #1 and #2, in both cases use secondary wires to route the signals to the logic analyzer.

3. Drive both behavior cameras with TTLs from the miniscope's DAQ "sync out" line. Use the Image Acquisition Toolbox in MATLAB (MathWorks) to collect TTL triggered video frames from each camera.
 - (a) Within the Toolbox's interface, remember to set Frames Per Trigger to 1 and to allow an infinite number of triggers. We recommend saving as a grayscale, uncompressed AVI as this allows easiest use by downstream analysis software. If hard drive space is an issue, make sure that you conduct a test recording and run it through downstream software before the first experiment to ensure you do not have codec compatibility issues. Run each camera on a separate computer if possible, to minimize the chance of dropped frames.
4. Use the second logic analyzer (SL8) to collect stimulus-onset times from a custom-designed circuit that allows you to select a stimulus and press a button to timestamp when you deliver each stimulus, this delivers a signal to the SL8 (Fig. 5d). Use the Saleae software (Logic 1.2.xx) to record and save all data from each SL8. We wrote custom Python and MATLAB scripts to extract the data from each Logic data file for use in subsequent analysis, *see* the below software:
 - (a) Use the CIAtah `saleae_stimulusFileConvertToMatlab.py` function after installing <https://github.com/ppannuto/python-saleae>.
5. After each imaging session, manually check each session's annotated stimulus-onset times. We use a custom MATLAB program interface to scroll manually through videos recorded from the camera positioned below the mouse. Your program should automatically find all times you pressed a button and move the video to that timestamp. This saves time from scrolling through the entire video and allows you to look in a defined time window around stimulus onset then correct instances in which the annotation did not match the actual onset time of stimulus delivery. *See* **Note 10**.
 - (a) **Note 10:** Determining stimulus onset time is critical for obtaining reliable and consistent data. Variability in this parameter can reduce sensitivity when trying to determine which neurons are part of the nociceptive ensemble. We recommend delivering the full stimulus set to a test mouse then looking through the recorded videos at stimulus onset times and come to a consensus on what you consider a successful stimulus delivery. These same criteria should

be used for all subsequent animals. For example, the first frame in which you see an indentation of the plantar surface of the hind paw is annotated as pin prick onset time.

In the second, alternative setup, use a series of Arduinos (three Unos and one Mega) to acquire the data and record the data using COM device recording software on a computer, for example in MATLAB or Python.

1. Make sure that your Arduino code outputs data to a computer with internal session times based off of each Arduino's internal clock as well as a frame counter from the miniature microscope frame number (via the TTL). Use the miniscope frame numbers to do the final synchronization in later analyses with the miniscope Ca^{2+} imaging data. Each data-collecting Arduino should receive a synchronizing TTL signal from the miniature microscope's DAQ.
2. Stream data to a PC and save it using a custom MATLAB script. We provide MATLAB code to read serial data from Arduinos, *see* the "saveArduinoCOMPort.m" function in CIAtah.
3. The miniature microscope DAQ should output a TTL that triggers an interrupt pin on an Arduino Uno, which then produces a 5 V output pulse on a separate port, driving each behavior camera and allowing you to synchronize each camera video frame with the Ca^{2+} imaging data. Alternatively, a BNC splitter can be used to directly send the miniature microscope output TTL to each camera, but this can at times lead to dropped frames.
4. Use a separate Arduino Mega to collect information on stimulus delivery times via a custom circuit that allows you to select the current stimuli, using a keyboard (Adafruit, Product ID #1824) and LCD display (Adafruit, Product ID #772), and to click a button upon stimulus application to record the delivery time for later analysis. Setup the keyboard and LCD according to guides on the Adafruit website. The button allows current to flow from a wire attached to a 3.3 V or 5 V line on one of the Arduinos to an interrupt pin, this allows precise detection of the button press without needing to use while loops in the code. In the code for this Arduino, output the timestamps of each miniscope frame along with timestamps whenever a stimulus is pressed.
5. Use a third Arduino Uno to measure the analog voltage signal from the accelerometer (Sparkfun ADXL335 or ADXL345) attached to the miniscope with a custom 3D printed attachment. Output a timestamp, and associated session frame number, of x , y , and z channel values at 100 Hz.

6. Use the last Arduino to measure the onset of licks and send control signals to open a solenoid (NResearch, 161P011) and release sucrose (10% w/v in water).
7. Conduct stimulus onset time correction identical to the alternative setup.

3.9 Behavioral Apparatus for Noxious Stimuli Delivery

We designed the behavioral apparatus to allow experimenters to easily gain access to the animal's paws while also being able to record neural and behavior activity to aide in downstream analysis. We recommend creating a behavioral apparatus that utilizes T-slotted framing and Thorlabs parts or similar construction materials, as detailed in Fig. 5c. This design and parts have several benefits: they are sturdy and thus less susceptible to movement when the experimenter bumps into the setup, allowing the animal to remain less disturbed; they allow for multiple points at which to anchor experimental devices; they are easy to disassemble and clean; and they allow flexibility to adjust positioning of supplemental devices like cameras and counter-balance arms.

1. Use either steel or aluminum perforated sheets and place on top of the T-slotted setup. We recommend aluminum as it does not rust and thus will be easier to clean over time.
 - (a) Do not use chicken wire or similar types of holed metal sheets as they contain numerous pressure points that might be painful to animals in certain experimental conditions; for example, those in which the animal has mechanical hypersensitivity, such as spared nerve injury.
 - (b) If you plan to have the electronics (detailed in the next section) or other items that you do not want contaminated by animal waste, make a 2nd metal sheet layer below the bottom behavior camera and place an absorbent sheet on that 2nd layer. This layer can also function as a place to put von Frey filaments and other stimuli for more rapid access.
2. Create plastic containers, where animals will be during experiments, that are either all transparent red or is white on all sides except for the front, which if possible should be red to reduce the ability for the animal to see the experimenter [25] while still allowing behavioral recording of the animal. Drill a small hole onto the left side of the container, this will be used to place the sucrose lick spout through.
3. While the miniscope only weighs a couple of grams, during a long experiment this can place unnecessary strain on the animal. We recommend using a counter-balance system to reduce the weight the animal carries, which will also allow you to get a better measure of nocifensive behaviors. Attach a counter-

balance arm (SMCLA, Instech labs) to the T-slotted system using Thorlabs posts then position the above the animal and container.

- (a) Before starting any experiment, loop the miniscope through the arm and test that the counter-balance arm's weight or spring is set to allow some give, but keeps the miniscope suspended, as this will reduce weight on the animal's head while still allowing it to move around freely.
4. Use two cameras to record mouse behavior and position one below the mouse, to capture stimulus delivery and reflexive responses, and another facing the test chamber, to capture the mouse's affective-motivational nocifensive behaviors. Follow the design in Fig. 5c.
 - (a) Take care that you focus the bottom camera on the animal's paw, as this will be crucial during analysis to help determine when stimuli have contacted in animal's paw.
 - (b) For low-light conditions or if the cameras do not have high sensitivity, purchase an infrared light and shine it on the paw area; this will allow you to better visualize the paw in the videos but will not affect animal behavior as rodents do not see in infrared.
 - (c) If there is a worry about animal moving out of focus, purchase a lens with (or adjust existing one to have) a high F-stop to allow more parts of the apparatus to remain in focus during experiments.

3.10 Recording Neural Activity During Delivery of Noxious Stimuli

The goal of these experiments is to identify neurons that are responsive to noxious (painful) stimuli. We term these noxious-stimuli responsive neurons the “nociceptive ensemble.” A second aim of these experiments is to have a set of control stimuli that reveal what percent of the nociceptive ensemble is unique to pain and which also respond to any (e.g., regardless of valence) salient, aversive, and other stimuli. This battery of tests will allow researchers to better understand what types of stimuli their brain region of interest responds to and whether using computational tools, they are able to disentangle what aspect of neural activity is pain versus nonpain related and how this activity changes in a chronic pain state.

1. After you mount the miniature microscope onto a mouse, check that the animal still has adequate GCaMP expression, either by using C1Atah to analyze the Ca^{2+} imaging movie recorded as the animal woke up from mounting or by running a 10-min open field imaging session. See Subheading 3.14 for details on analyzing imaging movies.

2. Habituated each mouse to the testing environment for at least three days prior to imaging (Fig. 6a). Each habituation session should last 20–30 min and take place in the same chamber as the final experiment. Use the light meter to ensure that the lux in the room is similar across days. *See Note 11.*
 - (a) Note 11: To preclude any emotional contagion between mice [26], we brought only one mouse into the isolated, light-, sound-, and temperature-controlled testing environment. Further, we housed mice individually after mounting to reduce probability that animals would chew on the baseplate, resulting either in a need to remount the animal or removing it from the experiment. Follow institutional guidelines and modify protocols accordingly if this is not possible. Isolating the animals may also be critical during chronic pain experiments, where housing naïve mice with those in chronic pain may lead to alteration of naïve mice’s behavior and neural activity.
3. Before starting the pain imaging sessions design a randomized stimulus delivery protocol for each session, subject to the following constraints: give a defined order to light touch, noxious cold, mild touch, and innocuous liquid or noxious heat at the beginning of each session; the same stimuli should not have adjacent stimuli blocks; and “Approach/No contact” stimuli blocks should occur during the first 3 main stimuli superblocks (Fig. 6b). *See Note 12.*
 - (a) Note 12: Having the first four stimulus blocks always occur in the same order across days allows you to track daily pain behaviors and the development of chronic neuropathic pain. All subsequent stimulus blocks are semirandomized computer-generated sequences within and across days with the condition that the same stimulus block does not occur twice in sequence, nor does the same daily protocol repeat on any given day. This ensures that neural responses are due to stimulus delivery rather than the animal expecting said stimulus or being put in a specific, stimulus-induced state over time. We designed this protocol to be less than 2.5 h for each animal’s imaging session; to give enough stimuli to have sufficient statistical power to identify stimulus-responsive neurons; and to incorporate sufficient “down time” between stimuli, in order to avoid potential photobleaching of imaging area or animal exhaustion. During “Approach” trials you will move either a von Frey filament, water droplet, pin, or noise device toward the animal similar to other trials but with no actual contact or stimulus delivery.

4. Turn on your cooling and heating devices and place a beaker of water on each. Allow each to reach 0 °C and 65 °C, respectively, and immerse the 1-mL syringes in each to equilibrate the temperature. This last step ensures that there will be minimal change of the water temperature toward baseline after removing the syringe from the water. If you are using acetone instead of cold water for cold stimuli, instead keep a vial of acetone ready next to the testing setup. Another alternative is to use dry ice [27].
5. At the start of each imaging session, head-fix the mouse (Siskiyou CC-1 clamp), mount the miniature microscope, check for GCaMP fluorescence, align the field of view (FOV) to the previous session FOV (*see Note 13*), take a picture of the current day's FOV, and place the mouse within the test chamber.
 - (a) *Note 13: It is very important that you spend the extra minute or two to get the FOV aligned as closely as possible to the previous days FOV, as that will be critical later on when attempting to align cells across imaging sessions. Alternatively, you can always align to the first day's FOV, this will minimize the chance of a slow drift of the FOV if you only align to the previous day's FOV; we prefer this method to ease later computational analysis. Further, we strongly recommend that you determine the size of the frame you will need to include the entire relevant FOV (e.g., 1000 pixels × 950 pixels) and keep this fixed for all experiments with that particular animal. This will greatly simplify downstream cross-session analysis.*
6. Clean the chamber and metal grating with 70% ethanol then place the mouse in the chamber and run the miniature microscope and accelerometer cable through a counter-balance arm placed above the chamber. This reduces the weight of the miniature microscope on the animal's head and reduces the probability that the cable will drop into range of the animals mouse (if that happens, animals may chew the cables).
7. Start the behavior video cameras and logic analyzers (Fig. 5a) so that they are waiting for a synchronization signal from the miniature microscope. At the start of each session, begin the miniature microscope recording and make sure that all other software and hardware is collecting correctly (Fig. 5b, c). Discard this data then setup all devices for the real experiment.
8. Before sensory stimulation, measure spontaneous neural activity by recording Ca^{2+} activity for 10 min while the mouse habituates to, and freely moves within, the testing box. The mouse should receive no explicit experimenter-delivered sensory stimuli during this period. However, in each session block,

record all stimuli, behavior camera, accelerometer, lick detection, and sucrose delivery signals (Fig. 5d) as this will simplify data analysis later.

9. After baseline recording, give the mouse 15 min ad libitum access to an incentive (sucrose) to capture neural responses to positive valence stimuli. To induce mice to lick without needing prior water deprivation, use a 10% sucrose solution. *See Note 14.*

- (a) You can detect licks and delivered sucrose using a custom-built circuit based on previous designs [24] and Fig. 5a. You will need to build a custom electronic circuit (built using Arduino elements) to collect lick data and synchronize all incoming data using output TTL pulses (5 V signals) from the miniature microscope DAQ (*see* Fig. 5a). Control signals from this circuit will drive a solenoid (NResearch, 161P011) that delivers 10% sucrose instantly after the 1st lick in a bout. Program a 5-s cool-down period between liquid deliveries. Thus, even if the mouse licks the port continuously, this approach provides enough time between incentive deliveries to relate the evoked neural activity with specific sucrose delivery time points.

- (b) Note 14: It is critical that the mouse should not be water- or food-restricted during any part of this protocol unless that is an intended experimental manipulation. In part, we want to minimize long-term water restriction as this protocol can take up to 2–3 months when including the chronic pain and negative valence studies. Further, as it is known that thirst and stress alter brain-wide neural dynamics [28, 29] and pain processing, the goal of this experiment is to minimize animal stress as much as possible to reduce confounds in downstream analysis and interpretation of the data.

10. Next, begin the main sensory testing protocol. Here you will deliver a battery of stimuli to the mouse's hind paw: 0.07-g and 1.4- or 2.0-g von Frey hairs (light and mild touch); 25-G needle (noxious pin prick); water drops at ~5 °C or acetone (noxious cold), 30 °C (innocuous liquid), and ~55 °C (noxious heat) delivered via applying a small drop from a 1-mL syringe; fake-out stimuli where no contact is made with the mouse after a stimulus device is placed near their hind paw ("Approach/No contact"); and noise (startle response control, delivered near the face). Deliver all stimuli at least 15 times per session, except "Approach/No contact" and noise, which you can deliver 9 times each. *See* Fig. 6 for detailed timing information. *See Note 15.*

- (a) Note 15: The number of stimuli to give for each stimulus should be determined based on the reliability of the neural activity seen in pilot studies. We used neural power analysis (run in a similar manner to common behavior power analyses) to determine how many stimuli we would need in order to observe significant, stimulus-responsive neurons at a specific power (e.g., 0.8). We give less of the control stimuli to reduce the length of the imaging session and in cases, like loud noise, where the neural activity is reliable.
 - (b) For von Frey and pin prick stimulation, attempt to hit the same lateral portion of the animal's hind paw to reduce variability and have a location that is still sensitive to mechanical stimulation after spared nerve injury (depending on which branches of the sciatic nerve are cut).
 - (c) For water or acetone delivery, we normally applied a 50–100 μL droplet onto the hind paw. Another option is to spray 100 μL onto the hind paw; however, this can lead to simultaneous mechanical stimulation.
 - (d) Include “Approach/No contact” trials to detect possible neural responses related to expectation of stimulus delivery and error-prediction. To conduct these “Approach/No contact” imaging trials, bring either an 0.07-g von Frey hair, a 25G needle, 1-mL syringe, or an 85-dB noise delivery device toward the animal but neither making contact nor turning on the noise. Randomly intersperse “Approach/No contact” trials between other stimuli blocks to ensure you capture any changes in anticipatory behavior that occurs as the session progresses.
 - (e) To control for the possibility that the neural responses to hind paw stimuli are startle-induced, use a loud tone ($\sim 80\text{--}85$ dB) as an aversive, but nonnociceptive, sensory stimuli. Deliver the tone (centered around 4 kHz in our experiments but can vary depending on the needs of your experiment and equipment availability) for 300 ms by triggering an Arduino, loaded with custom code, to drive a TDK PS1240 Piezo Buzzer. *See* many online tutorials for producing sound using Arduinos and Piezo buzzers.
11. While imaging neural activity, also measure withdrawal reflexes and affective-motivational behaviors (attending and escape) using high-speed cameras (AVT Guppy Pro F-125 1/3" CCD Monochrome Camera #68-567 or The Imaging Source DMK 23FM021) and accelerometers (Sparkfun ADXL335 or ADXL345, with data collected using an Arduino Uno or Saleae Logic 8). Wire them together as in Fig. 5a.

- (a) The accelerometer can be assembled using guides available on commercial websites for the products in Subheading 2. Connect the x , y , and z accelerometer channels to individual channels on the logic analyzer and in the acquisition software, set to acquire at 100 S/s. This ensures that you oversample behavior relative to miniscope data acquisition rate, which allows for more precise timing of behavior changes relative to neural activity.
12. We recommend between each superblock that researchers save data from the logic analyzers, miniature microscope, and behavior cameras. This prevents loss of a large amount of data in the case of electronic failure or accidents during the experiments. You can do this during the 3 min break periods between each super block (Fig. 6b).
13. At the end of each imaging session, remove the miniature microscope and return the animal to its home cage.

3.11 Miniature Microscope Recording Parameters

We recommend recording all miniscope videos at a frame rate of 20 or 30 Hz, especially if using GCaMP6m or a Ca^{2+} indicator with similar rise and decay kinetics. We typically use between 213 ± 3 and 390 ± 7 μW LED light intensity (measured from miniature microscope GRIN with a Thorlabs PM100D and S120C). Each frame from the Inscopix miniature microscope CMOS camera is 12-bit of varying video dimensions—we typically ran analysis on videos of size $250\text{--}275 \times 250\text{--}270$ pixels after downsampling in each spatial dimension by a factor of 4 from the raw data. Use a stage micrometer (Ward's Natural Science, 94W 9910) to empirically calculate the real-world dimensions of each video pixel by placing the miniscope on the holder from Subheading 3.4 and lower down until the micrometer is in focus then take a picture. In an image editing software, open the resulting image and measure the number of pixels between markers of known width, for example 100 μm . This will then allow you to calculate the pixels per micron for each miniature microscope used. In the case of the Inscopix nVista 2.0 miniature microscopes, this was typically $2.51 \mu\text{m} \times 2.51 \mu\text{m}$ per pixel.

3.12 Noxious and Aversive Stimuli Experiments

These experiments are similar to those in Subheading 3.8 and use the protocol outlined in Fig. 6c. The goal of these experiments is to determine how specific the nociceptive ensemble activity is to noxious (painful) stimuli as compared to other aversive stimuli.

1. Habituated mice to a fear conditioning test chamber, similar to prior setups [30], for 30 min on four consecutive days prior to conducting experiments.
2. Prepare the animals for imaging as in Subheading 3.8. Use 70% ethanol to clean all chambers and surfaces that animals will contact before each experimental imaging session.

3. After you mount the miniature microscope, habituate mice to the test chamber for 10 min.
4. After habituation, give mice 10 min of ad libitum access to 10% sucrose, record accelerometer, miniature microscope, stimulus delivery time, and behavior camera data during this time to facilitate easier downstream analysis.
5. Follow the protocol outlined in Fig. 6c and used the same data collection hardware as in Subheading 3.8.1. You will deliver a range of noxious, aversive, and appetitive stimuli to animals: noxious cold (acetone), noxious heat (~55 °C water), noxious pin (25G needle), air puff (300 ms), isopentylamine (~85 mM in H₂O, delivered via 300-ms air puff), loud noise (~85 dB for 300 ms, same as previously described), electric footshock (0.6 mA for 2 s), quinine (0.06 mM), and 10% sucrose.
 - (a) Deliver quinine last in the main stimulus chamber (before moving to the fear conditioning chamber) to reduce confounds by exposing the animal to a bitter, aversive stimuli before testing noxious and aversive stimuli. Give mice quinine (0.06 mM in deionized water [31]) after they lick a metal tube in an identical manner as 10% sucrose but through a different tube to avoid contamination by sucrose.
 - (b) Because the main behavior chamber and the fear conditioning chambers were in separate rooms, we allotted time for the mouse to rehabilitate to the fear conditioning chamber for 10 min after the ad libitum quinine access.
 - (c) Deliver noxious cold (acetone), noxious heat (~55 °C water), noxious pin (25G needle), and loud noise (~85 dB) as described in Subheading 3.8.
 - (d) Isopentylamine (Sigma-Aldrich SKU #126810, CAS #107–85-7) has an odor shown to be aversive in multiple previous studies [32–34]. Other odors are possible to use, just avoid using fox urine or any odors that might cause long-term changes in the room's odor and thus the animal's level of stress.
 - (e) To conduct isopentylamine and air puff experiments, place 50 µL of isopentylamine onto a small piece of tissue paper (Kimtech, #05511) and place it immediately into a 10-mL blood serum tube (Fisher # 02685A) and re-cap. Then insert two 16G needles through the tube cap and attach one of them using plastic tubing to a valve (Gems Sensors and Controls, MB202-VB30-L203) controlling air delivery. Deliver air by attaching the other needle to flexible tubing that leads to a metal tube or 16G blunt needle, which you will use to manually direct odorant to animals in the test chamber. Deliver air puffs through a

blunt, 16G needle, but bypass the odorant-filled serum tube; the best way to do this is to use a three-way stopcock to redirect airflow to a separate, empty tube with a needle at the end. We recommend delivering both isopentylamine and air puff for 300 ms with medical-grade compressed air (UN1002) at between 20 and 30 PSI. Aim the isopentylamine and air puff stimuli during delivery at the nose and front half of the animal's face, respectively.

- (f) For footshock trials, habituate mice for 10 min then deliver five 0.6-mA electric footshocks with 2 min between each stimulation (Fig. 8c, d). To synchronize the onset time of each footshock with Ca^{2+} imaging data and each behavior cameras' videos, collect TTLs output by the miniature microscope DAQ and footshock software (Freeze Frame, Actimetrics) on a logic analyzer (Saleae Logic 8), which allows you to determine the specific image frames of the Ca^{2+} video that were synchronous with each footshock.
6. Collect all data in this procedure, process the Ca^{2+} videos, and perform analyses as in the main protocol in Subheading 3.8.

3.13 Analysis of Locomotor Behavior in the Open-Field Assay

The open-field procedure serves two purposes: as a quantitative measure to ensure that the animals exhibit normal locomotor behavior after each surgery and as a control to determine how correlated with general locomotion a given brain area is, as this can affect interpretation of stimulus-evoked activity in Subheading 3.16.

1. Create an open field chamber that is either circular (60.96-cm D, 38.1-cm H, opaque white polyethylene walls and floor) or square (24" × 24" × 12", white opaque HDPE) using tape.
2. Habituate animals in the testing room for 5 min before starting the experiment. We recommend only having one mouse present in the room during all imaging sessions.
3. Conduct open field experiments either at 20–25 or 102 lux (measured with light meter) or at the same lux as the experiments in Subheading 3.8 using a diffuse overhead fluorescent light to illuminate the arena. Ambient room temperature should be ~26 °C. Place a camera above the chamber, load the Image Acquisition Toolbox in MATLAB, and position the chamber in the center of the camera frame. Crop any regions outside the chamber from the camera frame to save storage space. Using a BNC cable to connect the miniature microscope DAQ "sync out" TTL port directly to the camera (e.g., via a HIROSE cable if using The Imaging Source cameras).
4. Mount the miniature microscope on the animal as in Subheading 3.8. Start the video camera so that it is waiting on a trigger from the miniature microscope.

5. Wipe all surfaces down with 70% ethanol before each session then place individual mice in a black plastic container. Place this container in the center of the arena. This allows you to release the animal into the arena without having to touch them and gives you time to setup the imaging parameters while the animal calms down after mounting.
6. Release the animal facing the peripheral zone (e.g., the chamber wall) and immediately start the miniature microscope recording. Record for 15–30 min depending on your experimental needs. At the end of the session, remove the miniscope from the animal and return to the home cage.
7. Analysis is done as in [18, 35, 36]; the most important analysis is to compare the average population firing rate vs. specific velocity bins and look at the average population firing rate at the onset and offset of locomotion. See **Note 16**, the code and instructions for tracking animal position at https://bahanonu.github.io/calciumImagingAnalysis/help_animal_tracking.
 - (a) Note 16: Some brain regions are known to be highly correlation with locomotion, such as the striatum [35]. For these types of regions, additional care must be taken when interpreting stimulus-evoked activity as it is likely to be nonspecific and occur in response to any salient stimuli. Use control and aversive stimuli described in the main- and aversion-pain experimental protocols to help determine whether most stimulus-responsive neurons are in fact just locomotion related. Further, using the accelerometer, you can analyze portions of the pain imaging experimental sessions when animals exhibit movements that are of equal magnitude as those seen in response to experimenter-delivered stimuli and look at whether the activity of the neurons is on average above baseline during those periods. There are several ways to get around the issue of locomotion-induced activity masking the response to noxious stimuli. One is to perform the experiments under light anesthesia, which is not ideal as detailed in Subheading 3.6. Another possibility is to body restrain the animals, but this can cause stress and alter neural responses to noxious stimuli.

3.14 Preprocessing of Ca^{2+} Imaging Data

In this step we detail analysis of the Ca^{2+} imaging data collected in prior experiments. You can perform all the analysis steps in our open source *CIAtah* (pronounced cheetah, also known as calciumImagingAnalysis [*CIAPKG*]) software package. The code is located at <https://github.com/bahanonu/calciumImagingAnalysis> while and instructions for use can be found at <https://bahanonu.github.io/calciumImagingAnalysis>. We refer to *CIAtah* modules that correspond to each step using italics. We

processed all Ca^{2+} imaging data in the MATLAB software environment using methods similar to previous studies [13, 18, 30, 35]. You can perform many of the steps described below (semi-)automatically using CIAtah; we describe the algorithms and relevant details here in case the reader would like to replicate them using their own code or software environment.

1. To reduce computational processing times and boost signal-to-noise, downsample imaging movies collected from the miniature microscope in both x and y lateral spatial dimensions using 4×4 (or 2×2 if you prefer to retain spatial details) bilinear interpolation.
 - (a) Within CIAtah, run the *modelDownsampleRawMovies* module or perform spatial downsampling within the *modelPreprocessMovie* module.
2. To remove motion artifacts, register all frames in each imaging session to a chosen reference frame using *Turboreg* [37]. We often register to the 100th frame to avoid any LED warm-up or other artifacts that can occur in earlier frames in an imaging session. Select and register a sub-region of the field-of-view rather than use the entire frame for registration. This allows you to choose a region with stable, high-contrast features (e.g., blood vessels) and without artifacts (e.g., dust particles on the optics) that could impede registration. *See Note 17.*
 - (a) Note 17: To improve the performance of motion correction, we make a duplicate movie to obtain translation coordinates. First, normalize the movie by subtracting the mean value from each frame. Then, spatially bandpass-filtered each frame of the movie; we use a cutoff frequency of ~ 0.10 to 0.16 cycle/ μm using a Gaussian cutoff filter, which highlighted spatial features at the ~ 6 to 10 μm scale. Next, perform an image complement operation on each frame by subtracting each pixel value from the maximum pixel value in that frame (i.e., dark areas became light, and vice versa); this inverts the image and generally makes blood vessels and other dark static features appear more prominently, which benefits image registration. Then obtain the two-dimensional spatial translation, skew, and rotation coordinates from *Turboreg* by having the algorithm compare each processed frame to a reference frame (e.g., the 100th movie frame). Discard the duplicate movie used in this step to save memory.
3. To facilitate cell extraction by enhancing cell signals and diminishing neuropil and other background fluctuations, divide each frame of the raw Ca^{2+} movie by a low-frequency bandpass-filtered version of itself (cutoff frequency: ~ 0.0014 to 0.0063 or ~ 0.0014 to 0.01 cycle/ μm using a Gaussian cutoff filter).

- (a) We recommend users test their movies with the *CIAtah viewMovieRegistrationTest* module to determine what filtering parameters best reduce background fluorescence while maximizing cellular signals.
 - (b) It is important to conduct spatial filtering *before* transforming each image. The reason for this is that transformation often leads to 0 s or NaNs near the edges of the movie and this will often lead to errors or sub-optimal results when trying to apply a spatial filter (e.g., after a fast Fourier transform) to the movie.
4. Conduct an affine or projective transformation on the resulting image frames using the two-dimensional spatial translation, skew, and rotation coordinates obtained in **step 2**, but on the Ca^{2+} movie preprocessed in the manner described in **step 3**.
 - (a) In certain cases, if users perform multiple rounds of motion correction to improve results, the absolute transformation from initial to final image can be obtained by using the translation (T), skew (S), and rotation (R) transformation matrices to compute $D = \prod_1^N T_i * S_i * R_i$, where i is the iteration, N is the number of registration rounds, and D is the absolute transformation matrix. This can also be used when transforming cell ROIs during cross-session alignment.
5. Since motion correction can cause the movie edges to take on inconsistent borders filled with 0 s or NaNs due to variable translation distances, you should determine the maximum amount all frames were translated during the motion correction procedure in each dimension (t_{\max}) and then add a border of size t_{\max} pixels extending from the edge of each frame toward the middle of the frame. Set a maximum border size (t_{\max}) to ensure a single frame does not cause most of the movie to become a border, for example 14 pixels ($\sim 35 \mu\text{m}$ with Inscopix nVista 2.0).
6. Covert each movie frame to relative changes in fluorescence using the following formula: $\frac{\Delta F(t)}{F_0} = \frac{F(t) - F_0}{F_0}$, where $F(t)$ is frame at time t and F_0 is the mean image over the entire movie.
7. Next, temporally smooth each movie by downsampling from the original 20 or 30 Hz to 5 Hz. Specifically, for a $x \times y \times t$ movie, bilinearly downsample in $x \times t$ to reduce computational processing times, which is equivalent to performing a 1D linear interpolation in time of the intensity values at each pixel. Skip this step if you are in a brain region or performing an experiment in which higher temporal resolution is of paramount importance.
8. As an optional step, you can manually crop out regions of the movie that correspond to large artifacts (e.g., dust particles) or

regions outside the microendoscope. This will improve cell extraction and save manual cell sorting time by reducing sources of high variance noise within the movie.

9. You can perform these steps within the CIAtah *modelPreprocessMovie* and *modelModifyMovies* modules.

3.15 Extraction of Neuron Shapes, Locations, and Activity Traces

After processing each session's Ca^{2+} imaging videos, you want to computationally extract individual neurons and their activity traces. There are several options for extracting cell images and fluorescence activity traces from Ca^{2+} imaging movies. There is the widely used principle component analysis followed by independent component analysis (PCA-ICA) algorithm [22]. In addition there are several constrained nonnegative matrix factorization methods (e.g., CNMF and CNMF-E), which are part of the CaImAn software package [38]. You can use these and other cell-extraction algorithms using the CIAtah *modelExtractSignalsFromMovie* module, see **Note 18**. We will focus here on PCA-ICA, as it is a fast and well-established method for analyzing miniscope data.

1. **Note 18:** We recommend users process their data with multiple cell-extraction algorithms to ensure that their results are independent of whichever algorithm they used. Our CIAtah software package provides seamless support for many commonly used cell-extraction algorithms along with several new techniques (e.g., CELLMax and EXTRACT) that we and others will be releasing in the future. Further, CIAtah supports the Neurodata Without Borders: Neurophysiology (NWB:N) data standard for optical neurophysiology, which facilitates the use of your cell extraction data cross software pipelines and languages.
2. Run PCA-ICA cell extraction using the following parameters: $\mu = 0.1$, a maximum of 750 iterations, and request ~ 1.2 to $1.5\times$ the estimated true number of active cells in the field of view.
 - (a) The parameter μ is the relative weight of temporal information in ICA, and $\mu = 0.1$ indicates we performed a spatiotemporal ICA with greater weight given to the spatial than to the temporal skewness.
 - (b) If running PCA-ICA on an animal for the first time, we recommend running with $1.5\text{--}2.0\times$ the number of estimated cells. This will increase the likelihood that you detect most of the cells. Since our implementation of PCA-ICA orders outputs roughly in order of their signal-to-noise ratio (SNR), you can then plot various cell shape (e.g., size) and activity trace (e.g., SNR) features and determine by eye, or using a threshold, where these parameters start to change. This change point is likely around

the true number of cells in the movie. Rerun analysis for that movie with the new estimate and run all subsequent analysis for that particular animal with the new estimate, unless you have reason to believe based on observations in the movie that the number of active cells has gone significantly up or down.

3. PCA-ICA outputs a series of candidate spatial filters ($x \times y \times n$) and temporal traces ($n \times t$)—where n is the number of neurons, t is the frame, and (x, y) are spatial dimensions—associated with temporally varying sources, which you then need to manually verify as neurons.
4. An optional step is to use the CIAtah *viewCellExtractionOn-Movie* to view the cell images overlaid on the imaging movie. This allows you to visualize whether the cell-extraction algorithms are missing any cells and adjust the number of requested cells or cell elimination parameters accordingly.

3.15.1 Manual Neuron Identification

After performing cell extraction, a human scorer needs to manually check algorithm outputs for accuracy and removal of false positives. You can perform these steps in CIAtah using the *computeManualSortSignals* module GUI.

For each imaging session, load the CIAtah GUI that displays the spatial filter and activity trace of each candidate cell, along with the candidate cell's average Ca^{2+} transient waveform (Fig. 7a). The GUI also shows a maximum projection image of all output spatial filters (Fig. 2c), on which the GUI highlights the currently selected candidate cell. Example PCA-ICA neuron extraction outputs from a single mouse (same as in Fig. 2c, d) showing accepted and rejected ICA outputs (Fig. 7a). See **Note 19**.

1. **Note 19:** We manually classify all neurons from nonneuron cell-extraction candidates obtained from imaging data based on a variety of parameters, such as the filter shape, the event triggered movie activity (e.g., whether it conformed to prior expectation of one-photon neuron morphology and GCaMP activity), location within the imaging field of view (e.g., not within a blood vessel), and the shape of the transient having characteristic GCaMP dynamics. We did not use automated heuristics to further remove accepted neurons in our studies, but these can be used should you want to save time. In Fig. 7a, “Spatial filters” are the PCA-ICA output filters, “Activity in movie” is a 31×31 pixel square region cropped from the movie around the candidate neuron's centroid location during that candidate neuron's transients (black outlines are “Spatial filter” derived neuron contours), and “Activity traces” shows the mean (black) and per transient (gray) PCA-ICA activity of a candidate neuron from the imaging session.

Cell-extraction algorithms often yielded candidate sources with images and activity traces that look highly similar to those of real neurons but that are actually associated with neuropil or other sources of contamination in the movie. Thus, the CIAtah GUI interface includes a section to avoid including these false positives. Specifically, the GUI crops the movie to a 31 pixel \times 31 pixel ($\sim 78 \mu\text{m} \times \sim 78 \mu\text{m}$) region centered on the centroid of each candidate cell then creates movies containing 10 frames before and after the onset of an individual peak in the candidate Ca^{2+} activity trace to help visualize actual transient-related activity in the movie. The GUI creates up to 24 of these movies (users can adjust this value) for each output based on each output's highest signal-to-noise (SNR) peaks. It then spatially concatenates all of these movies associated with a specific cell extraction output to create a montage movie that allows you to view movie data associated with peaks in the activity trace for each output at once, which improves decision-making.

We recommend using several criteria to classify a cell extraction output as a neuron: minimal overlap of an output's spatial filter with blood vessels or other contaminating signal sources, resemblance of each output's spatial filter to a 2D Gaussian or an expected neuron shape based on prior knowledge (Fig. 7a, "spatial filters"), similarity of the spatial filter to activity within the movie and proximity of output's centroid to movie activity (Fig. 7a, "activity in movie"), and similarity of the average transient waveform to a typical Ca^{2+} transient waveform as observed using GCaMP6, such as a fast rise time followed by a slow decay (Fig. 7a, "activity traces").

Fig. 7 (continued) noxious and aversive stimuli, while a separate neuron population uniquely encodes nociception. Background is a negative control showing average response during random trial time points at least 10 s away from any defined stimuli. **(d)** Divergent neural populations encoding appetitive (10% sucrose consumption) stimuli versus the nociceptive ensemble. **(e)** To test out the specificity of the neuronal ensemble dynamics between stimuli, we constructed a nine-way naïve Bayes decoder. For cross-validation, we split data each round 70:30 between training and test datasets using 2 s from each trial. After training the decoder, it was run on the test neuron activity data and the predicted stimuli state compared to the actual stimuli delivered. The decoder was run through 50 rounds subsampling different sets of trials for use in training and test datasets. **(f)** We constructed a naïve Bayes decoder, as described in Subsection 3.16.2, and applied it to the noxious vs. aversive stimuli experiments ($n = 6$ mice, 1 session each). The decoder was then run on neural activity data for a new subset of stimuli and the actual stimuli at those frames compared to those predicted. We then normalized each actual stimuli column by the number of total actual stimuli to allow comparisons of how accurate the de-coder was. Better performance (red/orange) occurred on noise and 10% sucrose than on innocuous (light purple) or noxious (blue and dark purple) stimuli. Symbols in the off-diagonal indicate whether prediction of correct stimuli was significantly higher than prediction of that stimuli (Wilcoxon sign-rank, Benjamini–Hochberg)

3.16 Basic Analysis of Noxious-Stimuli Responsive Populations

This next section will cover basic analysis of noxious-stimuli encoding cells (Fig. 7b–d). A critical aspect of this analysis involves analysis of neural responses to nonnoxious stimuli (Fig. 7c, d). To determine which neurons significantly responded to a given stimuli, the philosophy taken here is to identify which neurons encode for a given stimulus [39] as well as using decoding analysis [40] to demonstrate this neural activity is predictive of which stimuli animals received at a given time in the session.

1. Load the stimulus event times and neural activity traces from Subheadings 3.8.1 and 3.15.
2. Conduct **steps 3–5** below for each stimulus given in an imaging session.
3. Take the neuronal activity data (e.g., PCA-ICA output traces) from a 2-s-post-stimulus interval for all trials. This involves creating a $n \times t \times f$ matrix, where n = number of neurons, t = number of trials, and f = number of frames per trial. Then convert the matrix into 1-s bins by taking the mean of each bin's $\Delta F/F$ activity.
4. For each cell, compare the binned stimulus-response activity values to those in an identically binned 2-s window from -5 s to -3 s before the stimuli, *see Note 20*.
 - (a) **Note 20:** We recommend this range to minimize the effect that anticipatory behavior or stimulus onset timing errors have on the baseline. If you observe large neural responses to “Approach, no contact,” then either rerun imaging session being more careful to approach the animal from an angle that is most likely to minimize anticipatory behavior or shift the prestimulus comparison window closer to stimulus onset to include that neural activity in the analysis. The later would essentially be looking for added responses beyond anticipatory that are induced by the stimulus.
5. Pool this activity across all presentations (or trials) of a specific stimulus and calculate a p -value for each neuron using a Wilcoxon rank-sum. Designate any neurons for which $P < 0.01$ as being significantly responsive to a given stimulus. Adjust this value depending on the SNR of cells in your experiment or if after checking whether identified cells are marked significant, they have stimulus-evoked responses in the range that you expect (Fig. 7b). *See Note 21*.
 - (a) **Note 21:** Consider using a one-tailed Wilcoxon rank-sum, which has more statistical power, if prior literature indicates that neurons in your area of interest have low firing rates and that you are unlikely to be able to observe true

decreases in Ca^{2+} activity in response to a stimulus. Make sure to justify this *before* starting your statistical analyses and state this in any methods [41].

6. We define the *BLA nociceptive ensemble* consists of neurons significantly responsive to noxious pin (25G needle), noxious heat (55 °C water), *or* noxious cold (5 °C water or acetone). Separately assign stimuli responsive neurons to the nociceptive ensemble for each animal's imaging sessions using the above definition.

3.16.1 Analysis of the Overlap in Neural Ensembles Responsive to Different Stimuli

Whether the overlap in neural populations active to separate stimuli are significant can be determined by looking at whether the neuronal ensembles responsive to two different stimuli are consistent with a hypothesis of statistical independent coding channels. This is important, as just looking at the percent overlap is not informative absent knowledge about the stimulus-responsive and total active neural populations. To test this hypothesis, you need to compute the likelihood that statistically independent assignments of cells' coding identities would yield the observed level of overlap in the two coding ensembles. There are two ways to calculate the expected level of overlap under an assumption of independence: using bootstrapping to estimate an empirical null distribution and compared the actual overlap to that or a newer, faster method we introduced to calculate an alternative, exact solution [18].

The idea behind the exact solution is that you calculate the extent to which the observed overlap was unexpected by chance. This is a specific instance of the classic statistics thought experiment of drawing without replacement balls from an urn containing black and white balls. In these studies, we have a population of N neurons and are seeking the probability, p , of having k successes (number of significant neurons for stimulus #2) in a population with predefined K successes (number of significant neurons for stimulus #1) in n drawings (number of significant neurons for stimulus #2).

To conduct the analysis, use the *hygecdf* and *hygestat* functions in MATLAB (or the equivalent in your language of choice) to calculate p and the expected number of overlap neurons given the actual number of significantly responsive neurons observed for stimuli #1 and #2 (say, noxious heat and cold). You can validate this method obtains accurate results by comparing to shuffle tests based on the same parameters and using 1000 rounds of 1000,000 shuffles to construct bootstrapped distributions. Specifically, each shuffle consists of randomly rearranging the vectors containing 1's and 0's, with the number of 1's matching the number of stimulus-responsive neurons, indicating which cells are significant for each stimulus then comparing them to get the overlap. Do this 1000,000 times to get a distribution then calculate the fraction of values that are greater than the actual overlap value. Do this 1000

times to get a distribution of p -values. We demonstrated [18] that the two methods attained nearly identical results and thus we strongly recommend using the hypergeometric distribution instead of shuffle tests to reduce computational processing times and to obtain an exact p -value.

To determine whether the overlap in coding ensembles becomes more expected than chance, either before or after spared nerve injury, perform a Wilcoxon rank-sum tests using a Benjamini–Hochberg multiple comparisons correction [42] to identify whether the overlap differed significantly that expected by chance. You can obtain the expected overlap by using *hygestat*.

3.16.2 Decoding of Stimuli Based on BLA Neuron Activity

To test the specificity of the neural code in response to various stimuli delivered to animals, you can implement one of many classifiers. We have previously used naïve Bayes classifiers [18] and general linear model (GLM) decoders [35] to predict stimuli or behavior based on neural activity. You can implement both in the MATLAB programming environment using standard MATLAB libraries and toolboxes. In the below procedure, we will describe the use of Naïve Bayes classifiers, which assume statistical independence between predictors (i.e., neurons), but also work well when this is not strictly the case [13]. The goal of a naïve Bayes classifier is to predict the response, y (stimuli given at time point t) based on predictors, x_{1-n} (neurons), where n is the number of neurons in our case. Formally,

$$P(y(t), |x(t)_1, \dots, x(t)_n) = \frac{P(y(t))P(x(t)_1, \dots, x(t)_n|y(t))}{P(x(t)_1, \dots, x(t)_n)}$$

where t is a particular poststimulus frame during the session, $P(y(t))$ is the probability of a stimulus at a given time point, $P(x|y)$ is the probability of activity in neurons (x) given a stimulus (y) was present, and $P(x)$ is the probability of a neuron being activated at time t . Thus $P(y|x)$ gives you the probability of stimulus y given you observe x activity pattern within the entire neural ensemble. Then use the following classification rule under the assumption of statistical independence between predictors (e.g., neurons or x):

$$\hat{y}(t) = \arg \max_y P(y(t)) \prod_i^n P(x_i(t)|y(t))$$

This rule allows you to predict at each time point, t , the most likely stimulus (class of $\hat{y}(t)$) given the observed response of all n neurons. Procedurally, the steps are as follows, see Fig. 7c.

1. Split the neural data into testing and training sets on a per trial basis with 70% of trials for training and 30% for testing.
2. Perform a 50-fold cross validation by training a new decoder using randomly chosen set of training trials and testing that decoder on a nonoverlapping set of test trials sampled from the entire set of stimuli trials. See **Note 22**.

- (a) Note 22: Since you are creating decoders that must simultaneously predict either nine (Fig. 6b) or ten (Fig. 6c) stimuli, you need to avoid introducing biases in the test and training sets due to some stimuli having more trials than others. To correct for this, limit the number of each stimuli's trials used for testing and training to whichever stimuli in that session has the minimum number of trials. However, still allow sampling from the full range of trials for each stimulus during each test round.
3. For the training set, construct a $n \times f$ predictor matrix consisting of all n neurons in a session and f frames composed of all ten frames in a 2 s window after stimulus delivery for all trials and stimuli. Construct the response as a $I \times f$ vector composed of the same 2-s window after the stimulus for all chosen stimuli trials, marked with 1 s to indicate which stimuli trial each frame was associated with. For example, frame 450–455 mark with a 2 (for noxious heat) and frame 900–905 mark with a 3 (for noxious cold).
4. Next, use the predictor matrix and response vector to train a naïve Bayes classifier using the *NaiveBayes* MATLAB class with a Gaussian distribution assumed for $P(x(t)_1, \dots, x(t)_n | y(t))$, seen as below, where μ_y and σ_y are the mean and standard deviation estimates of neuron i response to a particular class (e.g., stimuli) in y .

$$P(x(t)_i | y(t)) = \frac{1}{\sqrt{2\pi\sigma_y^2}} \exp\left(-\frac{(x(t)_i - \mu_y)^2}{2\sigma_y^2}\right)$$

5. Next, run each trained classifier on another $n \times f$ matrix containing the test set neural activity data, this will give you an output of naïve Bayes classifier predictions of which stimulus trial is associated with each time point f .
6. Take the resulting predictions and compare to the actual given during those test set time points. One way to visualize this is to construct a confusion matrix from the predicted and actual stimuli then normalize each column (corresponding to each actual stimuli) by the number of actual stimuli given to allow comparison of the decoder accuracy for each stimulus compared to others, see Fig. 7f.
7. To ensure that the decoding specificity is due to an individual neurons' specific activity in response to each stimulus, run another 50 rounds where you shuffle the stimulus identities (e.g., $I \times f$ response vector in **step 3**) used to train the decoder but keep the testing set stimuli unchanged. This should remove much of the predicted stimuli specificity.

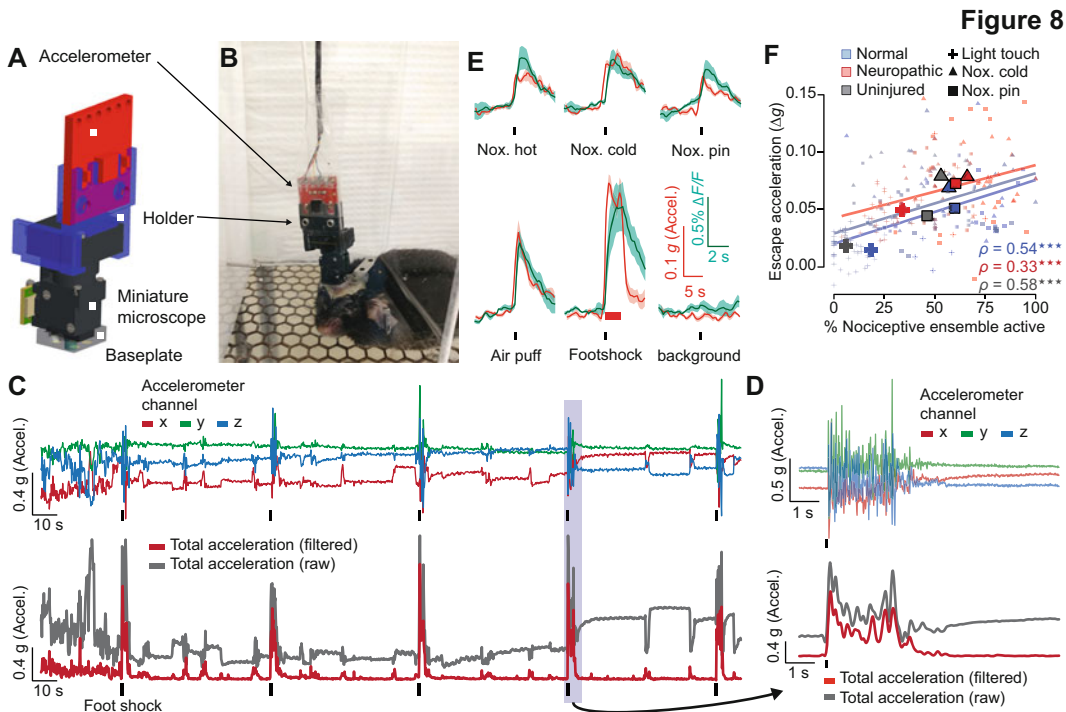


Fig. 8 Accelerometer-based recording of nocifensive behaviors. (a) 3D CAD model of the accelerometer (red) and 3D printed holder (blue) attached to the miniature microscope. (b) Picture of (a) in an experiment. (c) Example raw accelerometer traces for x , y , and z channels from an aversion experiment where a foot shock was delivered. Bottom traces show the raw acceleration and after filtering to remove artifacts (e.g., static component of gravity). (d) Zoomed in view of shaded region in (c). (e) Temporal dynamics of the mean $\Delta F/F$ of neurons within the nociceptive ensemble (cyan) and mean affective escape acceleration (red) for all imaging sessions and mice ($n = 6$ mice, 1 session each). (f) Correlation between % of nociceptive ensemble activated and escape acceleration per imaging session (light colored points) and across animal groups and conditions (dark, larger points) show significant correlation (Spearman's $\rho = 0.54$ [Normal], 0.33 [Neuropathic], and 0.58 [Uninjured])

3.16.3 Analysis of Accelerometer Traces

This section describes collecting and analyzing quantitative measurement of animal movement in response to stimuli using a triaxial accelerometer (Sparkfun, ADXL345 or ADXL335 accelerometer). The accelerometer is attached to the miniature microscope body by a custom 3D-printed part (Stratasys Objet30 printer, VeroBlack-Plus material, Fig. 8a). The `computeAccelerometerOutput` C/Python function helps with processing the accelerometer data.

1. Using a soldering iron, connect the accelerometer x , y , z , power, and ground lines to a multiwire cable. If using an Arduino, connect the x , y and z lines to analog inputs 1–3, respectively. If using a Saleae logic analyzer, connect to inputs 0–2. In both cases, connect the accelerometer to a 3.3 V power line and ground on an Arduino. Slot the accelerometer into the 3D-printed attachment and secure in place with setscrews before sliding onto the miniature microscope (Fig. 8a, b).

2. Collect accelerometer x , y , and z channel data using either a Saleae logic analyzer (Logic 8, 100 Hz sample rate, preferred method) or an Arduino running custom code (100 Hz sample rate). Synchronize each with Ca^{2+} imaging data using TTL pulses from the miniature microscope DAQ box (Fig. 5a).
 - (a) Store the output voltage from the accelerometer for later analysis at 10-bit resolution (1024 value range, for both Arduino and Saleae setups).
 - (b) For accelerometer data recorded at 100 Hz, downsample to 20 Hz by slicing the 100 Hz data into 50 ms bins and taking the mean value within each bin.
3. To remove noise in each accelerometer channel, use a median filter (4 frames wide) on each channel.
4. Since without using an accelerometer with a gyroscope you will not know the orientation of the accelerometer at all times, and to remove the static acceleration due to gravity [43], you should high-pass filter (zero-phase third-order Butterworth, 0.5-Hz cutoff frequency) the entire accelerometer x , y , and z channel digital signal.
5. Compute the total acceleration (A_t) using the below equation where a_x , a_y , and a_z indicate the x , y , and z accelerometer output channels (Fig. 8c, d).

$$A_t = \sqrt{(a_x)^2 + (a_y)^2 + (a_z)^2}$$

6. To further reduce noise, zero-phase lowpass filter the total acceleration (butterworth, 1 Hz cutoff, 3rd order).
7. Downsample the resulting total acceleration from 20 Hz to 5 Hz by binning the 20 Hz data into 200 ms sections and calculating the mean acceleration within each section.
8. For displaying the magnitude of change in behavior from baseline after a stimulus is given (Fig. 8e), it is at times preferable to use Z-scored acceleration instead of in units of g . In this case, calculate the mean (μ_{pre}) and standard deviation (σ_{pre}) response for 3–5 s before the stimuli (using the stimulus vectors constructed in Subheading 3.8.1) and compute the Z-score for the 5 s before and after the stimuli using the below equation where t is the frame relative to stimulus onset.

$$Z_{\text{score}}(t) = \frac{A_t(t) - \mu_{\text{pre}}}{\sigma_{\text{pre}}}$$

9. To determine whether animals have moved statistically more than chance, either before or after spared nerve injury, calculate the mean session response per animal in a 2-s window after each stimulus and compared it to a baseline from 3 to 5 s before each

stimulus using a Wilcoxon rank-sum test with Benjamini–Hochberg multiple comparison correction for the multiple stimuli being tested.

10. To ensure accuracy of the accelerometer recordings, compare accelerometer data for each stimulus to human scored data (*see* Fig. 2e) by calculating the % of that stimuli's trials in a session the animal scores as responding to a stimulus and compare this to the mean acceleration for that stimuli across all trials in the same session.
 - (a) We have found that the two measures are highly correlated (Spearman's $\rho = 0.79$, p -value < 0.001) and that the accelerometer offered a greater dynamic range to separate noxious stimuli that otherwise saturate near 100% of trials responsive with the binary measure of behavior used by humans.
11. After calculating the mean acceleration for each animal's session across all stimuli, compare the result to the percentage of neurons for a given stimulus that make up the nociceptive ensemble to see whether the degree of activation of "pain" neurons correlates with increased vigor in locomotion (Fig. 8f). Remember to compare these results to control locomotion experiments as outlined in Subheading 3.13, to reduce the possibility that these are really locomotion-related signals.

3.17 Cross-Day Analysis of Neuronal Activity

There is much interest both within the broader neuroscience community as well as within the pain field as to how stable neurons are in the stimuli they respond to and information they encode. With respect to pain, this is of interest both in terms of understanding how the nervous system relays nociceptive information to the brain (e.g., using labeled line, population coding, or another Schemes [44]) and has therapeutic implications: if the nociceptive ensemble is stable across time that would likely lead to an easier therapeutic target than an ensemble that is constantly changing (Fig. 10d, right). Further characterization of a stable ensemble might thus reveal a genetic component that leads to targeting of specific receptors (e.g., GPCRs) expressed by that stable population to help alleviate pain. Thus, to match neurons across days we will describe a multistep algorithm (Fig. 9) that expands on prior work [13, 18, 30]. Run the method on your data using the *CIAtah computeMatchObjBtwnTrials* module or *matchObjBtwnTrials* function. Below we describe the procedural steps for users who want to better understand the method or recreate using their own routines or programming environment.

1. Load the cell extraction spatial filters and threshold them by setting to zero any values below 40% the maximum for each spatial filter and use these thresholded filters to calculate each

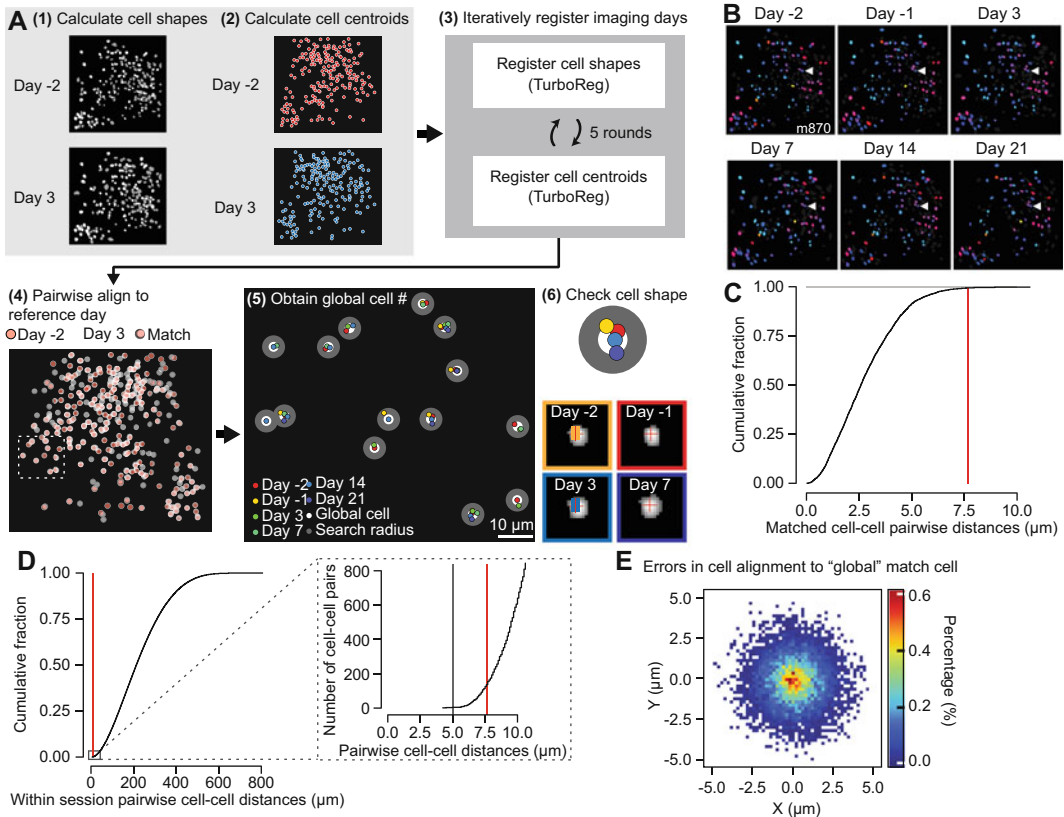


Fig. 9 Cross-session alignment of cells. **(a)** Method for cross-day alignment of neural ensembles using real data from an example mouse. Day -2 and 3 are with respect to nerve injury surgery day. After neurons had been matched (steps 4 and 5), they were associated with a global cell that was then used to analyze their responses across days. See text for detailed procedure. Red crosses in (step 6) are the global neuron centroid overlaid on the cell filters. **(b)** Example neuron spatial filter maps showing cross-day alignment for an example mouse's imaging sessions. Global cells matched across at least 70% of the imaging sessions are coded by a unique color. White arrow points to a neuron active across all aligned days for that animal. Scale bars, $100\ \mu\text{m}$. **(c)** Pairwise centroid Euclidean distances restricted to neuron–neuron pairs within the same global cell for all mice ($n = 17$), demonstrating the majority of neuron matches assigned to the same global cell are less than $5\ \mu\text{m}$ apart. Red line is at the same location as the 99.99th percentile in **(d)** inset. **(d)** Same calculation as in **(c)** for all imaging sessions across mice ($n = 17$) showing that the vast majority of neurons are $>10\ \mu\text{m}$ apart. Inset, zoomed in view showing the absolute number of neuron pairs within $10\ \mu\text{m}$ of one another. Red line indicates 0.01th percentile. Grey line indicates threshold used to group neurons in **(a)** into a global cell. **(e)** Individual neuron distances from their respective global cell centroid location if they were matched to another neuron on at least one other session ($n = 13,558$ session neurons)

neuron's centroid location. You can calculate the centroid using the *regionprops* function in MATLAB. Do not round each neuron's centroid coordinates to the nearest pixel value as this would reduce accuracy of cross-day alignment.

- Next, create simplified spatial filters that contained a 10-pixel-radius circle centered on each neuron's centroid location. This

allows you to register different days while ignoring any slight day-to-day differences in the cell extraction algorithm's estimate of each neuron's shape even if the centroid locations are similar.

3. For each animal, we recommend that if you have N sessions to align that you choose the $N/2$ session (rounded down to the nearest whole number) to align to (*align session*) in order to compensate for any drift that may have occurred during the course of the imaging protocol.
4. For all imaging sessions create two neuron maps based on the thresholded spatial (Fig. 9a, step 1, "thresholded neuron maps") and 10-pixel-radius circle (Fig. 9a, step 2, "circle neuron maps") filters by taking a maximum projection across all x and y pixels and spatial filters (e.g., a max operation in the third dimension on a $x \times y \times n$ neuron spatial filter matrix, where n = neuron number).
5. You then need to register these neuron maps to the *align session* using *Turboreg* [37] with rotation enabled for all animals and isometric scaling enabled for a subset of animals in cases where that improves results. The registration steps are as follows (Fig. 9a, step 3):
 - (a) Register the thresholded neuron map for a given session to the *align session* threshold neuron map.
 - (b) Use the output 2D spatial transformation coordinates to also register the circle neuron maps.
 - (c) Then register the circle neuron map with that animal's *align session* circle neuron map.
 - (d) Apply the resulting 2D spatial transformation coordinates to the thresholded neuron map.
 - (e) Repeat this procedure at least five times.
 - (f) Lastly, use the final registration coordinates to transform all spatial filters from that session so they matched the *align session's* spatial filters and repeat this process for all sessions for each animal individually.
6. After registering all sessions to the *align session*, recalculate all the centroid locations (Fig. 9a, step 4).
7. Set the *align session* centroids as the initial seed for all *global cells* (Fig. 9a, step 5). Global cells are a tag to identify neurons that you match across imaging sessions.
 - (a) For example, global cell #1 might be associated with neurons that are at index number 1, 22, 300, 42, and 240 within the cell extraction analysis matrices across each of the first five imaging sessions, respectively.

8. Starting with the *align session* for an animal, calculate the pairwise Euclidean distance between all global cells' and the selected session's (likely 1st) neurons' centroids.
9. Then identify any cases in which a global cell is within 5 μm (nominally ~ 2 pixels in our data) of a selected session's neurons. This distance depends on the density of cells in your imaging sessions, a stricter cutoff should be set for more dense brain areas, *see* Fig. 9d. When you find a match, then check that the spatial filter is correlated (e.g., with 2D correlation coefficient) above a set threshold (e.g., $r > 0.4$) with all other neurons associated with that global cell (Fig. 9a, step 6).
10. If a neuron passes the above criteria, add that neuron to that global cell's pool of neurons then recalculate the global cell's centroid as the mean location between all associated session neurons' centroid locations and annotate any unmatched neurons in that session as new candidate global cells.
11. Repeat this process for all sessions associated with a given animal.
12. After assigning all neurons across all animal's imaging sessions to a global cell, conduct a manual visual inspection of each animal's cross-day registration results. We recommend removing imaging sessions that did not align well with other sessions associated with a particular animal; while this leads to a loss of data the mis-aligned session can have detrimental effects on the cross-session algorithm's performance.
13. To quantify alignment accuracy, you should calculate the pairwise distance between all session neurons' centroid locations that are associated with a common global cell. Most alignments should be below 5 μm displacement from the global cell centroid (Fig. 9c, e).
 - (a) Use the `CIAtah computeCrossDayDistancesAlignment` module after running `computeMatchObjBtwnTrials` to obtain these numbers in a CSV table.
14. To calculate the number of sessions a global cell responded to specific stimuli (Fig. 10a), use the classification of significantly coding neurons found in Subheading 3.16. Create a $n \times s$ matrix where n = number of global cells and s = session, in which each matrix cell indicates 1 if a cell significantly responds on that session or a 0 if not.
15. Then check for each global cell the number of sessions it responds to a given stimuli while ignoring any global cells who only had activity on a single session.
16. To calculate maximum duration of time that a cell maintains responses to a given stimulus, use the actual date (since imaging sessions might not have been run on the exact dates

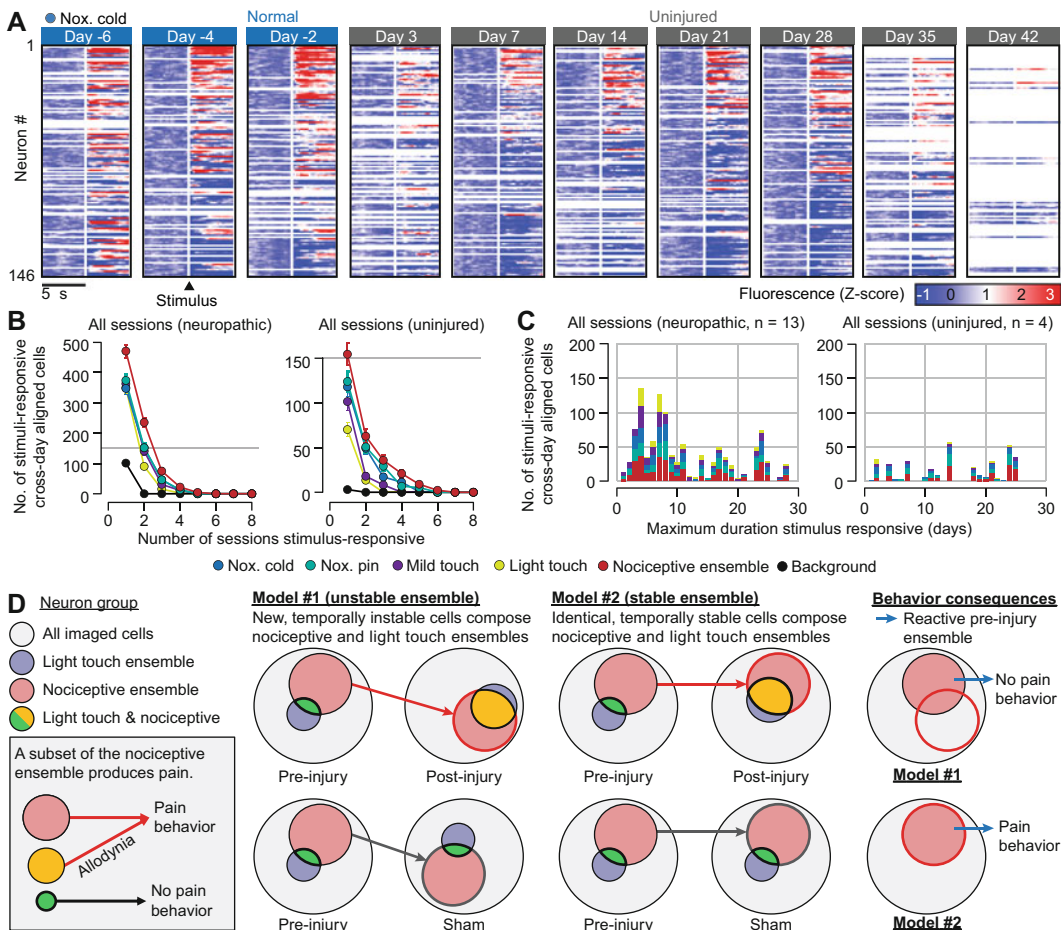


Fig. 10 Longitudinal analysis of the nociceptive ensemble. (a) Example animal showing all global cells ($n = 146$) that were active during greater than half of that animal's imaging sessions. A subset of neurons (top rows) are stimulus responsive to noxious cold (acetone) across multiple imaging sessions and days to weeks of time. Black sections indicate sessions in which no associated neuron was found for that global cell. (b) Indicates number of global cells that significantly coded for indicated stimuli (see Fig. 7b) across either one or more imaging sessions irrespective of temporal distance separating imaging sessions. Gray line is 150 global cells and is common across the neuropathic (top row) and uninjured (bottom row) imaging groups. "Nociceptive ensemble" stimuli are a global cell that responded to either noxious pin and/or noxious cold on any given imaging session. (c) To determine how long global cells coded for specific stimuli (color-coded), actual imaging session dates were used to calculate the maximum duration a global cells was found to be stimulus responsive. Of the 3223 global cells matched across two or more imaging sessions, ~11% (350 global cells) responded to noxious stimuli with at least a week separating their first and final noxious stimuli responses. (d) Two potential models of BLA nociceptive ensemble activity evolution following injury. In model #1, if the nociceptive ensemble changed cell identities across time and was identifiable on any given day, the cross-day analysis would show that the cells responding to light touch in a neuropathic state are different from the cells constituting the nociceptive ensemble cells preinjury. Regardless, if the neuropathic light touch ensemble is more similar to the neuropathic nociceptive ensemble (see orange shaded area), this would suggest that when observing each ensembles' activation, they are more overlapped between ensembles, suggesting that the animal may abnormally perceive the light touch stimulus as more aversive, or painful, than is warranted based on the nonnoxious character of the physical stimuli. In contrast, in model #2, the same effect would be observed except that the cells would be stable across time. This can be tested by using techniques to reactivate the preinjury ensemble and observe whether pain behavior is observed when those same cells are reactivated on later days (rightmost column)

specified in the Fig. 5 protocol) the imaging session took place on to calculate both the earliest and latest date that a global cell significantly responded to each stimuli. Take this difference as a measure of how long a neuron stably coded for said stimuli (Fig. 10b, c).

4 Outlook and Conclusions

The power of miniscope calcium imaging approach lies in its ability to link individual and population nociceptive neural activities to real-time nocifensive behavior. This opens the door to reevaluate several classic theories of how the brain computes and integrates a wide-range of sensory, contextual, and internal-state information into perceptions of pain. No doubt, the advantages of this optical recording approach come with several limitations and room for improvement. While the current class of genetically encoded calcium sensors has been one of the largest catalysts of contemporary neuroscience, calcium activity remains a proxy for action potentials and subthreshold electrical activity that carries immensely important information for understanding brain network dynamics. On the horizon are new genetically encoded voltage sensors that will improve this area, but the adoption of high-speed cameras, improved optics, multiphoton laser light sources, and improve computational and storage pipelines will need to parallel the use of voltage indicators before they can be widely used in the pain neuroscience community. Additionally, light-sensitive neural activity-indicators can be combined with light-sensitive opsins to turn pain-relevant circuits on or off at will. Using a closed-loop all-optical optogenetic-imaging approach could provide even further control for the reading and writing of pain-associated neural activity with tight anatomic resolution and subsecond precision. Nevertheless, the caveats and limitations of one-photon miniscope calcium imaging, as with any emerging technology, should be carefully considered and incorporated into your unique experimental designs and data analysis needs. Investigations into the neural circuits of pain-processing in the brain can now leverage this powerful tool to reverse translate the remarkable depth of key human brain imaging's results by drilling into specific brain regions to visualize the coding principles of nociceptive information and to identify, potentially, pain-specific neural pathways in the brain.

References

1. Basbaum AI, Bautista DM, Scherrer G, Julius D (2009) Cellular and molecular mechanisms of pain. *Cell* 139:267–284
2. Baliki MN, Apkarian AV (2015) Nociception, pain, negative moods, and behavior selection. *Neuron* 87:474–491
3. Devor M (2013) Neuropathic pain: pathophysiological response of nerves to injury. In: Wall and Melzack's textbook of pain. Elsevier Saunders, pp 861–888

4. Apkarian AV, Baliki MN, Geha PY (2009) Towards a theory of chronic pain. *Prog Neurobiol* 87:81–97
5. Pizzo PA, Clark NM, Carter Pokras O (2011) Relieving pain in America: a blueprint for transforming prevention, care, education, and research. In: Institute of Medicine. National Academies Press, p 382
6. Baliki MN, Geha PY, Fields HL, Apkarian AV (2010) Predicting value of pain and analgesia: nucleus accumbens response to noxious stimuli changes in the presence of chronic pain. *Neuron* 66:149–160
7. Baliki MN et al (2012) Corticostriatal functional connectivity predicts transition to chronic back pain. *Nat Neurosci* 15: 1117–1119
8. Guenther C, Miyamichi K, Yang HH, Heller HC, Luo L (2013) Permanent genetic access to transiently active neurons via TRAP: targeted recombination in active populations. *Neuron* 78:773–784
9. Dhawale AK et al (2017) Automated long-term recording and analysis of neural activity in behaving animals. *eLife* 6:e27702
10. Romyantsev OI et al (2020) Fundamental bounds on the fidelity of sensory cortical coding. *Nature* 580:100–105
11. Corder G et al (2017) Loss of μ -opioid receptor signaling in nociceptors, and not spinal microglia, abrogates morphine tolerance without disrupting analgesic efficacy. *Nat Med* 23: 164–173
12. Ghosh KK et al (2011) Miniaturized integration of a fluorescence microscope. *Nat Methods* 8:871–878
13. Ziv Y et al (2013) Long-term dynamics of CA1 hippocampal place codes. *Nat Neurosci* 16: 264–266
14. Kim TH et al (2016) Long-term optical access to an estimated one million neurons in the live mouse cortex. *Cell Rep* 17:3385–3394
15. Stringer C, Pachitariu M (2019) Computational processing of neural recordings from calcium imaging data. *Curr Opin Neurobiol* 55: 22–31
16. Stringer C et al (2019) Spontaneous behaviors drive multidimensional, brainwide activity. *Science* 364:255–255
17. Ahanonu B (2018) calciumImagingAnalysis: a software package for analyzing one- and two-photon calcium imaging datasets. GitHub
18. Corder G et al (2019) An amygdalar neural ensemble that encodes the unpleasantness of pain. *Science* 363:276–281
19. Paxinos G, Franklin KB (2019) Paxinos and Franklin's the mouse brain in stereotaxic coordinates. Academic
20. Jackman SL et al (2018) Silk fibroin films facilitate single-step targeted expression of optogenetic proteins. *Cell Rep* 22:3351–3361
21. Hua T et al (2020) General anesthetics activate a potent central pain-suppression circuit in the amygdala. *Nat Neurosci* 23:1–15
22. Mukamel EA, Nimmerjahn A, Schnitzer MJ (2009) Automated analysis of cellular signals from large-scale calcium imaging data. *Neuron* 63:747–760
23. Sorge RE et al (2014) Olfactory exposure to males, including men, causes stress and related analgesia in rodents. *Nat Methods* 11:629–632
24. Slotnick B (2009) A simple 2-transistor touch or lick detector circuit. *J Exp Anal Behav* 91: 253
25. Peirson SN, Brown LA, Potheary CA, Benson LA, Fisk AS (2018) Light and the laboratory mouse. *J Neurosci Methods* 300:26–36
26. Langford DJ et al (2006) Social modulation of pain as evidence for empathy in mice. *Science* 312:1967–1970
27. Brenner DS, Golden JP, Gereau RW IV (2012) A novel behavioral assay for measuring cold sensation in mice. *PLoS One* 7:e39765
28. Allen WE et al (2019) Thirst regulates motivated behavior through modulation of brainwide neural population dynamics. *Science* 364: 253–253
29. Livneh Y et al (2020) Estimation of current and future physiological states in insular cortex. *Neuron* 105(6):1094–1111.e10
30. Grewe BF et al (2017) Neural ensemble dynamics underlying a long-term associative memory. *Nature* 543:670–675
31. Blednov YA, Cravatt BF, Boehm SL, Walker D, Harris RA (2007) Role of endocannabinoids in alcohol consumption and intoxication: studies of mice lacking fatty acid amide hydrolase. *Neuropsychopharmacology* 32:1570–1582
32. Kobayakawa K et al (2007) Innate versus learned odour processing in the mouse olfactory bulb. *Nature* 450:503–508
33. Root CM, Denny CA, Hen R, Axel R (2014) The participation of cortical amygdala in innate, odour-driven behaviour. *Nature* 515: 269–273
34. Saraiva LR et al (2016) Combinatorial effects of odorants on mouse behavior. *Proc Natl Acad Sci* 113:E3300–E3306

35. Parker JG et al (2018) Diametric neural ensemble dynamics in parkinsonian and dyskinetic states. *Nature* 557:177–182
36. Li Y et al (2017) Neuronal representation of social information in the medial amygdala of awake behaving mice. *Cell* 171:1176–1190. e1117
37. Thévenaz P, Ruttimann UE, Unser M (1998) A pyramid approach to subpixel registration based on intensity. *IEEE Trans Image Process* 7:27–41
38. Giovannucci A et al (2018) CaImAn: an open source tool for scalable calcium imaging data analysis. *bioRxiv*, 339564
39. Quiroga RQ, Panzeri S (2009) Extracting information from neuronal populations: information theory and decoding approaches. *Nat Rev Neurosci* 10:173–185
40. Rolls ET, Treves A (2011) The neuronal encoding of information in the brain. *Prog Neurobiol* 95:448–490
41. Ruxton GD, Neuhäuser M (2010) When should we use one-tailed hypothesis testing? *Methods Ecol Evol* 1:114–117
42. Benjamini Y, Hochberg Y (1995) Controlling the false discovery rate—a practical and powerful approach to multiple testing. *J Royal Stat Soc B* 57:289–300
43. Mathie MJ, Lovell NH, Coster ACF, Celler BG (2002) Determining activity using a triaxial accelerometer. In: *Proceedings of the second joint 24th annual conference and the annual fall meeting of the biomedical engineering society*. IEEE, pp 2481–2482
44. Craig A (2003) Pain mechanisms: labeled lines versus convergence in central processing. *Annu Rev Neurosci* 26:1–30